

Voltage Source Multilevel Inverters with Reduced Device Count: Topological Review and Novel Comparative Factors

Ahmed Salem, *Student Member, IEEE*, Huynh Van Khang, Kjell G. Robbersmyr, *Senior Member, IEEE*, Margarita Norambuena, *Member, IEEE* and Jose Rodriguez, *Fellow, IEEE*

Abstract—Multilevel inverters have gained increasing interest for advanced energy-conversion systems due to their features of high-quality produced waveforms, modularity, transformerless operation, voltage and current scalability, and fault-tolerant operation. However, these merits usually come with the cost of a high number of components. Over the past few years, proposing new multilevel inverters with a lower component count has been one of the most active topics in power electronics. The first aim of this work is to update and summarize the recently developed multilevel topologies with a reduced component count, based on their advantages, disadvantages, construction, and specific applications. Within the framework, both single-phase and three-phase topologies with symmetrical and asymmetrical operations are taken into consideration via a detailed comparison in terms of the used component count and type. The second objective is to propose a comparative method with novel factors to take component ratings into account. The effectiveness of the proposed method is verified by a comparative study.

Index Terms—Multilevel inverter (MLI), symmetric operation, asymmetric operation, comparison factor, component for each level (CEL), single-phase, three-phase, DC-AC converter.

I. INTRODUCTION

Multilevel inverters (MLIs) have been developed for more than five decades and gained increasing importance in industrial applications as one of the most attractive solutions for implementing medium-/high-voltage high-power converters [1-13]. The MLIs are configured by a distinct arrangement of single/several DC sources, namely batteries, rectifiers, flying capacitors, fuel cells, PV panels, and semiconductor devices, e.g. insulated-gate bipolar transistor (IGBT), metal-oxide-semiconductor field-effect transistor (MOSFET), and diodes, in a way to produce a near sinusoid voltage with low distortion. Combining low-voltage DC sources with semiconductor switches can efficiently generate high-voltage stepped waveforms at the output of converters. The rating of the switches is defined by the rating of linked DC sources, so the voltage stress on the switches is much lower than the output voltage. From the 1970s, Baker and Bannister in [14] have invented the first converter topology, which is widely

known as cascaded H-bridge (CHB) MLI, using several DC sources. Each source was linked to a single-phase inverter to form one cell. By connecting more cells in cascade as shown in Fig. 1 (a), a multilevel output can be achieved. A few years later, in the 1980s, a single source multilevel topology called diode clamped or neutral point clamped (NPC) MLI has been proposed by Baker in [15]. Despite using one DC source, it requires several diodes that are connected to a neutral point, as shown in Fig. 1(b). In 1981, Nabae et al. in [16] have presented the NPC implementation by using the pulse-width modulation (PWM) scheme. Fig. 1 (c) shows a flying capacitor (FC) or capacitor-clamped MLI, being introduced during the 1990s in [17] and [18] by Meynard et al. and Lavieville et al., respectively. Although it needs only one DC source, several flying capacitors result in increasing both size and control complexity of the FC-MLI. These three topologies have considered as the basic MLI topologies in literature [1-4]. The DC-to-AC conversions using MLIs are widely used in power systems, transportation, and renewable energy systems, for example, in flexible AC transmission systems (FACTS) [19, 20], high-voltage direct-current (HVDC) [21, 22], active power filters (APFs) [23, 24], variable frequency drives (VFD) [25-27], pumped storage power plants (PSPP) [28-30] and grid-connected or standalone PV systems [31-33].

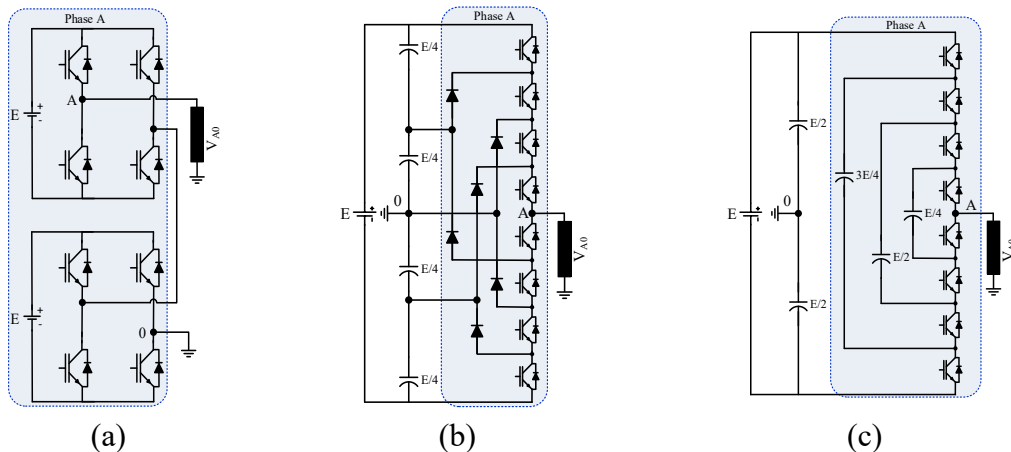


Fig. 1 One leg of the basic MLI topologies for five-level configurations. (a) CHB MLI. (b) NPC MLI. (c) FC MLI.

The MLI based DC to AC converters have several attractive merits as reported in [1-13]: A) producing high-quality waveforms with low harmonic contents and low dv/dt stress, significantly reducing the total harmonic distortion (THD), filter dimensions, and electromagnetic interference (EMI). B) operating in both fundamental and low frequency switching schemes can lower switching losses, being beneficial for efficiency and cooling requirement, especially in high-power applications. C) using low-rated standard semiconductor devices for producing high voltage without connecting them in a series manner as in two-level medium-power inverters. D) having small/zero common-mode voltage (CMV) can eliminate drawbacks of CMV in many applications, for example, the stress in the bearing of a driven motor fed by MLIs can be reduced in drive systems. Moreover, several MLIs have further strategic merits, namely transformerless operation,

modularity, voltage and current scalability, high redundancy in switching states, and fault-tolerant operation. On the other hand, these merits come with the cost of a high number of passive and active components, such as DC sources, flying capacitors, inductors, diodes, and switches. Consequently, the volume, cost, and complexity of the inverter are increased [1-13]. Thus, proposing new MLIs, that can enlarge the level number along with a low component count is currently one of the key research trends in this research theme [3, 11]. Within the theme, improving efficiency, power density, control simplicity, reliability, cost, and broadening MLIs applications have attracted a large number of publications every year. Accordingly, reviewing the most advanced knowledge in this research field periodically is always of importance to update the research baselines or the newest reflections, resulting in many review studies presented in [1-13]. Most of those studies give a detailed review of MLIs based on a specific application or inverter family, e.g. transportation [8], medium-voltage drives system [13], modular MLIs [5-9], HVDC applications [10], and renewable energy integration [3]. Moreover, the existing reviews have used two conventional factors, namely the level-number per switch ratio (LSR) or component per level factor (CLF), to assess the component counts among topologies [34, 35], which are not able to take component ratings or cost and stresses of component into consideration.

To address the problem of existing comparative factors, this work proposes a novel comparative factor, so-called "component for each level (CEL)", in addition to a review of the most promising MLI topologies. Unlike the existing reviews focusing on a specific application, this work reviews diverse MLI topologies in a wide range of applications. Further, a comparative study is presented to verify that the proposed factor allows comparing the component count among MLIs more efficiently.

The rest of this paper is organised as follows: recently proposed voltage source multilevel inverters will be classified and reviewed in Section II in detail, while both existing and the proposed methods for comparing MLIs will be discussed in Section III. Finally, conclusions are drawn in Section IV.

II. CLASSIFICATION OF MULTILEVEL INVERTERS

The recently developed MLI topologies are subdivided into three main groups based on the number of phases, i.e. single-phase, three-phase, and over-three-phase configurations as shown in Fig. 2. The selected topologies are allocated in different subgroups, namely single DC source, multiple DC sources, symmetrical MLIs, asymmetrical MLIs, transformer-based, and transformerless MLIs. The first two main groups are the main focus of this paper, being detailed in the following sections.

A. SINGLE-PHASE MULTILEVEL INVERTERS

This section presents a detailed review of the recently developed single-phase MLI topologies (or groups C2 and C1 in Fig. 2) in terms of construction, features and limitations. The addressed topologies are applied in renewable energy, motor drives, and power systems with diverse designs and characteristics. This review focuses on the MLI with a boosting capability, coupled inductors-based MLI,

transformers-based MLI, specially designed topologies for particular applications and hybrid unipolar MLI topologies.

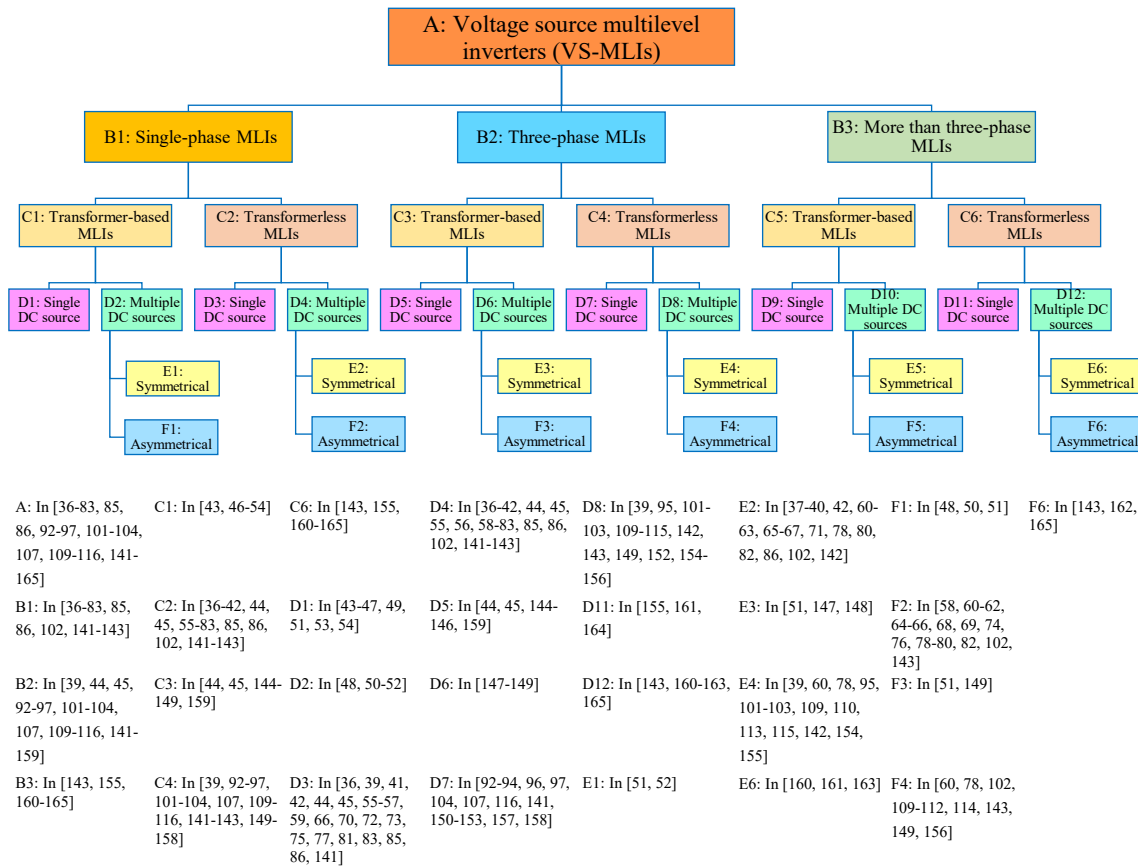


Fig. 2 Classification of multilevel voltage source inverters.

A novel single-phase MLI with the boosting capability is proposed in [36] as shown in Fig. 3, consisting of three stages, conventional boost converter, switch-diode-capacitor cell, and full H-bridge inverter. These three stages function as a step-up, level generator, and inversion stages, respectively. It can produce five voltage levels by using a single DC source, three power diodes, two capacitors, six switches, and an input inductor. Unlike other five-level inverters, the topology's main features include boosting capability, using a single DC source and low switch count. However, bulky size, high losses and limited lifetime are still a problem since it requires capacitors, inductor and a significant number of diodes. This circuit is suitable only for low-voltage applications because of high-voltage stress across the switches of the used H-bridge. To overcome these limitations, a quasi-cascaded H-bridge configuration was proposed in [37] as illustrated in Fig. 4 (a), consisting of two cascaded modules for generating five levels. Each module has one DC source, one inductor, one capacitor, two diodes, and four power switches. The problem of limited generated voltage was solved by using modules in a cascaded configuration. To improve the performance of the topology under unbalances of the DC sources, resulting in a voltage difference in the existing capacitors, and a DC offset at output, an additional capacitor C_d has to be used

between modules as shown in Fig. 4 (b). Although this capacitor has a low-voltage rating, it must carry the entire load current.

Other C2-group MLIs based on coupled inductors have been presented in [38-40]. In [38], a π -type MLI was proposed for single-phase applications. Additionally, the upgrading possibility for three-phase applications was discussed in [39]. The π -type MLI consists of two three-terminal switch network (SN) as illustrated in Fig. 5 (a), each SN is configured by using two switches and two diodes. The five-level circuit uses two DC sources, two capacitors, four diodes and two coupled inductors. The coupled inductors are connected in series, and the connection point produces the output node A, while the outer terminals B and C are connected to the middle points of SNs. One of the key advantages of the presented topology is using only four switches for producing five voltage levels $+E/2$, $+E/4$, 0 , $-E/4$, and $-E/2$ without using any flying capacitor, resulting in control simplicity with a moderate size. However, lack of modularity and using coupled inductors limit the applicability of the proposed circuit. Belong to the same family, four nine-level coupled inductors-based topologies were proposed and analysed in [40]. Figs. 5 (b), (c), (d) and (e) show the suggested circuits, being formed by using two DC sources, switches, and pairs of coupled inductors. They have the common limitations of topologies in [38, 39], but do not use any diode or capacitor.

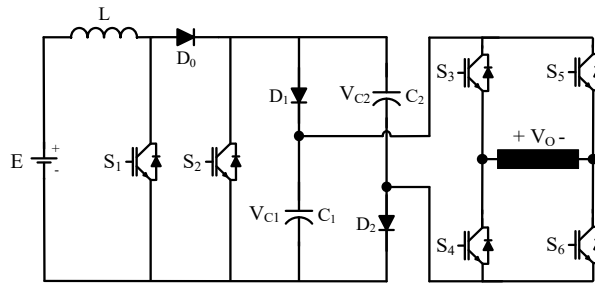


Fig. 3 Enhanced single-phase step-up five-level inverter [36]. Capacitor's voltage (V_{C1} , V_{C2}) = $E/(1 - D_{S1})$, where D_{S1} is the duty cycle of S_1 .

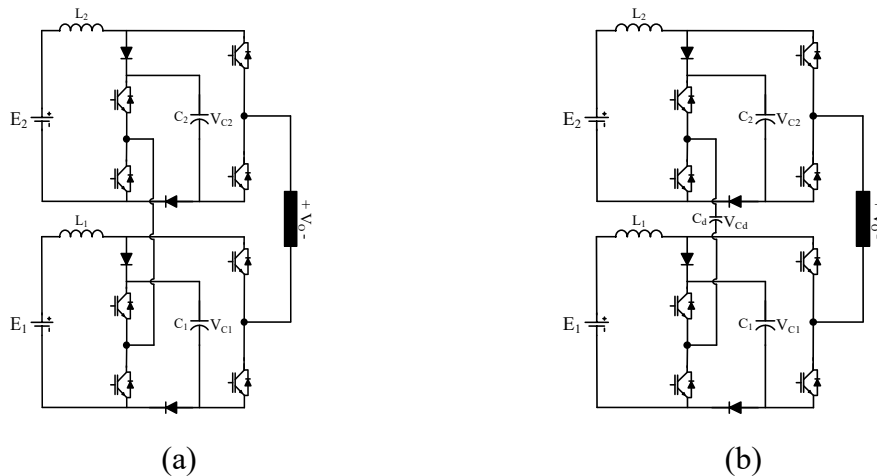


Fig. 4 Quasi cascaded H-bridge five-level boost inverter [37]. $V_{C1} = E_1/(1 - 2D_1)$, $V_{C2} = E_2/(1 - 2D_2)$, and $V_{Cd} = (D_1 - D_2) V_{(C1 \text{ or } C2)}$, where D_1 and D_2 are the shoot-through duty cycles.

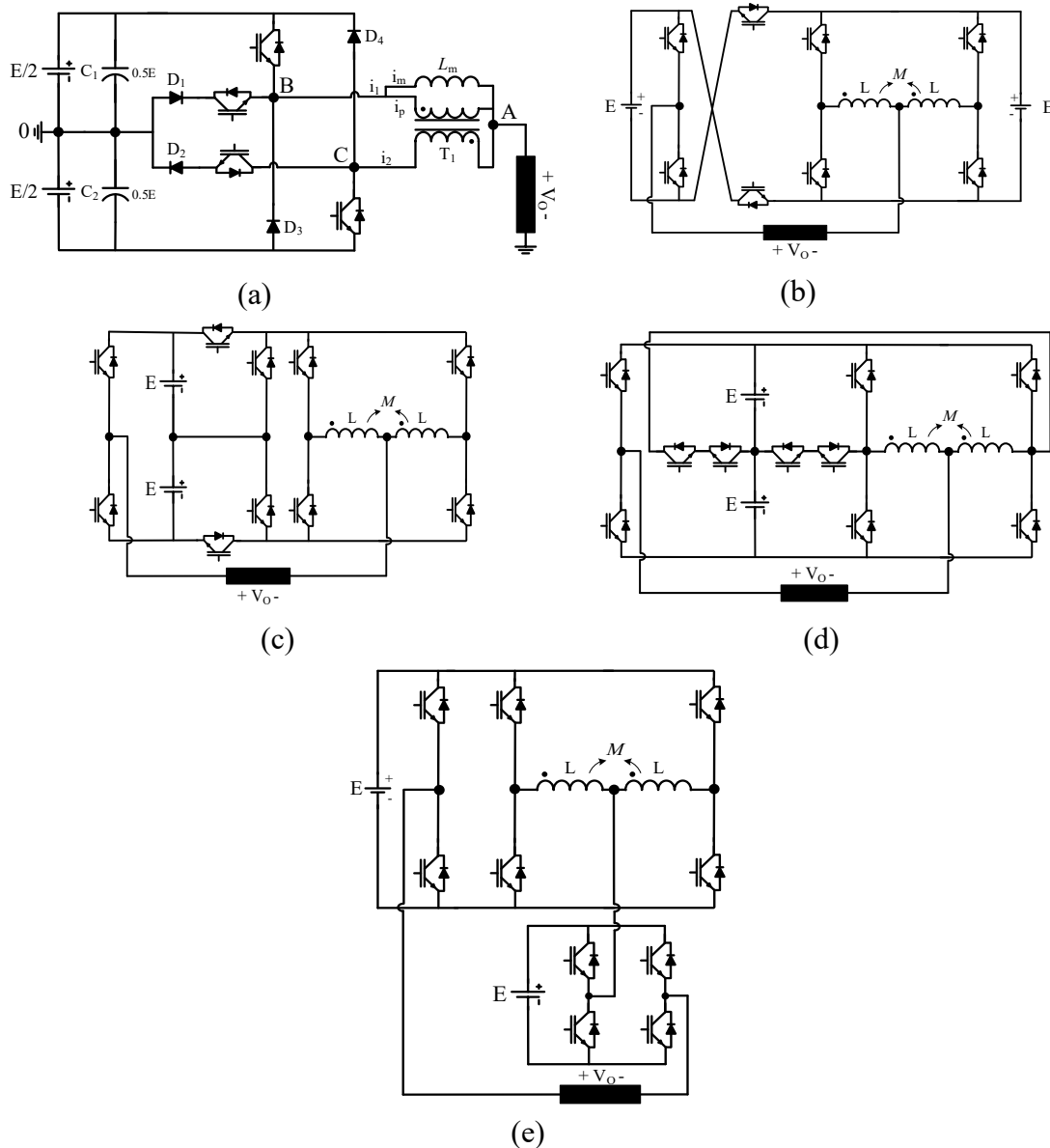


Fig. 5 Multilevel single-phase inverters with a pair of coupled inductors [38-40]. (a) Single-phase π -type five-level inverter [38, 39]. (b) Active series voltage sources with coupled inductors (AS-CI) [40]. (c) Active neutral point clamped with coupled inductors (ANPC-CI) [40]. (d) Extended ANPC-CIs (EANPC-CIs) [40]. (e) Cascaded with coupled inductors (C-CIs) MLI [40].

Two-hybrid MLI topologies were proposed in [41, 42], being formed by connecting three-level flying capacitor-fed-H-bridge (FCHB) cell with either three-level T-type cell in [41] or three-level active neutral-point-clamped (ANPC) cell in [42]. Connecting the FCHB cell with T-type or ANPC cells generates only five voltage levels of $-E/2$, $-E/4$, 0 , $E/4$, and $E/2$, with a peak value equal to half of the DC-link voltage (i.e. $0.5E$). Consequently, a two low-frequency switches (LFS) cell was recommended by the authors in [41, 42] to increase the peak value and level count of the output voltage. The peak value becomes E (i.e. the full DC-link voltage), and the level count is enlarged to nine levels instead of five (the additional four levels are: $\pm E$ and $\pm 3E/4$). Fig. 6 shows the nine-level configurations of the presented topologies in [41] and [42]. Fig. 6 (a) illustrates the presented topology

in [41], consisting of three capacitors, ten switches, and one DC source, while the introduced topology in [42] requires twelve switches, three capacitors and one DC source for producing nine voltage levels as depicted in Fig. 6 (b). The two topologies have the same count and rating of the capacitors (two of $E/2$ and one of $E/4$), the switches in the LFS (two of E), and FCHB (four of $E/4$) cells, but they require different switch counts and ratings of the utilised switches in ANPC and T-type cells. The presented topology in [42] needs two more switches as compared to the topology in [41]. Although the switches of ANPC and T-type cells have the same total standing voltage (TSV) of $3E$, they have different voltage ratings. All switches in the ANPC cell have the same voltage rating of $E/2$, while the switches in the T-type cell have different voltage ratings (two of E and two of $E/2$). From the industrial point of view, using switches of equal ratings is better than having different ratings, in terms of maintenance, manufacturing, and loss/temperature distribution, making the presented topology in [42] more advantageous than the presented topology in [41]. It is worth mentioning that the level count can be enlarged for both topologies by connecting additional FCHB cells. In [42], two methods were suggested (can be applied for the topology in [41] as well): either keeping a single DC source while repeating the FCHB cell or cascading the structure in Fig. 6 (a) (or Fig. 6 (b) for the topology in [42]) to construct a multiple DC source configuration. The two extension methods can be used as depicted in Fig. 6 (c) for gaining more benefits, depending on the availability of DC sources and the required output voltage. Using a single DC source and the possibility for generating a higher number of voltage levels by adding FCHB cells are the main features of these circuits, beside using a low component count. However, requiring a significant number of different rating capacitors for enlarging the voltage level count increases the inverter footprint and control complexity. Moreover, using the two-switch cell across the DC link makes these topologies more applicable in low-voltage applications alone.

Theoretically, the modularity feature enables producing an infinity number of voltage levels with high-voltage values by using low-rating semiconductors but requiring a higher number of components. In this direction, the cascaded transformer multilevel inverter (CTMLI) family (or C1 group in Fig. 2) has been proposed for eliminating the needs for numerous numbers of DC sources and floating capacitors while suffering the cost of required transformers [43-54]. Figs. 7 (a), and (b) show the conventional CTMLI, and a reduced component version was reported in [43]. The conventional topology uses four switches tied with a low-frequency transformer as a building cell, while the circuit in Fig. 7 (b) merges two cells to save almost half of switches count. Modularity, employing a single DC source, capacitor- and diode-free are the main merits while using bulky low-frequency transformers is the main demerit.

In [55-68], several topologies (belong to group D3 and D4 in Fig. 2) have been proposed for producing multilevel voltages as shown in Figs. 8, 9, and 10. All of them use two stages, one for generating unidirectional multilevel DC voltage and the other one for changing the polarity of the generated voltage from the first stage

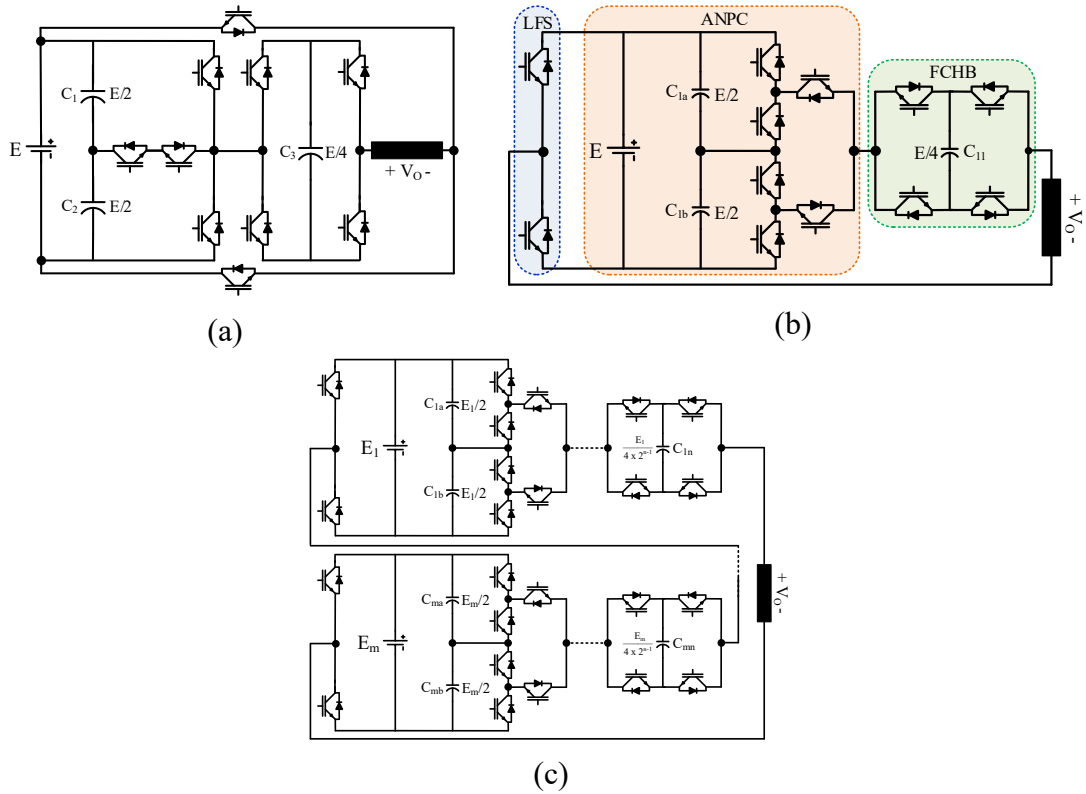


Fig. 6 Improved hybrid MLI topologies [41, 42]. (a) Nine-level inverter with reduced part count [41]. (b) Nine-level configuration of the double-hybrid ANPC inverter [42]. (c) N -level configuration for the double-hybrid ANPC inverter [42].

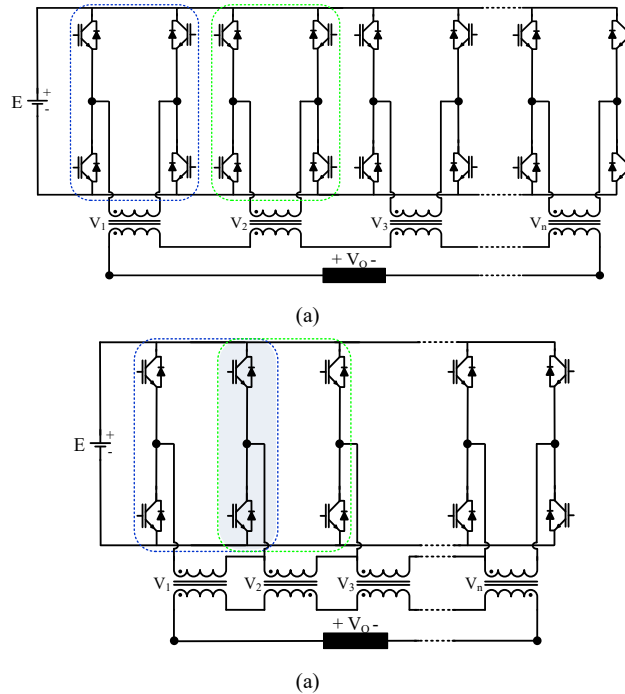


Fig. 7 Cascaded-transformer multilevel inverter (CTMLI) [43]. (a) The conventional CTMLI. (b) Low component merged cells CTMLI in [43].

to multilevel AC voltages. This common technique for obtaining AC voltage makes the mentioned circuits suffered from high-voltage stresses across the switches in the second stage, reducing the permissible operating voltage and limiting them to low-voltage applications. For example, the topology in [55] uses a new switched-capacitor (SC) as the first stage while a normal full H-bridge acts as a polarity changer stage for obtaining nine levels. Fig. 8 (a) shows this topology, having a reduced component count and the ability to avoid the voltage balance problem by the inherent self-voltage-balance feature. Therefore, the switching algorithms get simplified. Despite using one DC source, it requires two capacitors, two power diodes, and nine switches with different ratings for generating nine levels. By using a new quasi-resonant SC (QRSC) circuit instead of the existing SC in Fig. 8 (a), a new QRSC multilevel inverter has been developed in [56]. It allows producing N voltage levels by increasing the number of the capacitors, but it has high-voltage stress across the switches of the H-bridge, lowering the input DC source voltage. Further, the self-voltage balancing feature can be realised by fully connecting the capacitors in parallel or partially to the load or source. Because of this connection, current spikes appear, increasing the capacitance, and decreasing the inverter lifetime. To overcome this challenge, the quasi-resonant inductor in the QRSC circuit is used to suppress these spikes, reducing the capacitance and prolonging the expected lifetime. Fig. 8 (b) shows N -level version of QRSC topology, requiring one DC source, one inductor, X capacitors, X diodes, $2X+2$ switches, where $X = (N-1)/2$.

The proposed topology in [57] uses several unidirectional and bidirectional modules for building different substages, working as a level-generator stage. The H-bridge is to change the voltage polarity as demonstrated in Fig. 8 (c), in which a single source inverter uses nine capacitors and 42 switches for producing 49 levels. Although the proposed circuit does not use any inductor, it can boost the low input voltage to a high value. The output voltage is limited only by the voltage rating of the H-bridge four switches. For example, the voltage stress across these four switches will be $24E$ for $N = 49$ levels, where E is the input voltage. Boosting feature is obtained by charging several capacitors stage by stage in a cascaded manner, i.e. the capacitors of the current substage can be charged by the capacitors of the previous substages. Using a single low DC voltage source for producing high voltage levels is the main merit of this topology, in addition to the diode-, inductor-free features. However, using many capacitors (nine for the 49-level version) with different capacitances and voltage values makes the control schemes complicated, decreasing the reliability and lifetime of the converter. An improved topology based on this circuit has been published in [58], having almost the same structure for the first two stages except replacing the two capacitors by two DC sources. For the last stage, it uses several full H-bridge cells instead of only one in [57], avoiding using the single-phase H-bridge to change the voltage polarity or high-voltage switches to obtain the negative voltage levels. Fig. 8 (d) shows the complete configuration, producing 55 voltage levels by using seven capacitors, 44 switches and three asymmetrical DC sources.

Fig. 8 (e) shows a new single-source seven-level topology investigated in [59], in which three-level DC-voltages are produced by using level-generator stages,

consisting of a single DC source, three capacitors, four switches, and four diodes, Moreover, a traditional H-bridge was used for producing the negative part, being more suitable for low-voltage applications alone. Using only one DC source is counted as an attractive advantage of this topology, but it has limitations regarding using diodes and capacitors as mentioned before. For example, to overcome the challenges for keeping the voltage of the capacitors in the DC-link balanced, the authors in [59] have recommended to use a resonant switched-capacitor unit (RSCU) as highlighted in Fig. 8 (e), increasing complexity, cost and the inverter size.

A new switched-capacitor MLI (SCMLI) was proposed in [60], which shares the same shortcomings like the topologies in [55-59] while using a new six-switch configuration for changing the polarity instead of using H-bridge. Further, multiple asymmetrical DC sources are used instead of using a single source, and voltage generator cells are required for generating multiple DC link voltages. Each one consists of two switches, one capacitor, one diode, and DC source. A 17-level version of the proposed MLI is shown in Fig. 9 (a), requiring ten switches, two capacitors, two diodes, and two isolated DC sources having asymmetrical values of E , and $3E$, respectively. To increase the output levels with a reduced component count, several topologies in the same family were proposed and summarized in Figs. 9 (b)- (h), being detailed in [61-67]. As seen from Figs. 9 (b)- (h), their key characteristics are realised as diode-, capacitor- inductor-free, boosting capability, using only a single DC source, a high number of capacitors, inductors and DC sources. However, they suffer from a common drawback, i.e. using polarity-changer stage, making the output voltage limited by the rated voltage of the switches.

A recently developed member of the unipolar MLIs family was proposed in [68]. Fig. 10 (a) shows the nine-level asymmetric structure of this topology, consisting of a unipolar level generator part followed by a conventional H-bridge cell to obtain bipolar multilevel voltages, similar to the topologies in [55-67]. Fig. 10 (a) shows the proposed topology, in which two trinary asymmetrical DC voltage sources ($E_1:E_2$ is 1:3) and ten switches are necessary for producing nine voltage levels of $4E$, $3E$, $2E$, E , 0 , $-E$, $-2E$, $-3E$, and $-4E$. As suggested by the authors in [68], the voltage level count can be enlarged to 3^X levels by adding $(4X+2)$ switches and 'X' DC sources as depicted in Fig. 10 (b). The proposed topology has remarkable merits, namely reduced component counts, and being capacitor-, and inductor-free. However, the high total standing voltage of switches in both level generator and polarity changer parts is considered its main demerit. For example, the switches of the polarity changer H_1 - H_4 must block the full dc-link voltage (i.e. $E_1+E_2+\dots+E_X$), in addition to the different high-voltage stress across the remaining switches based on their location in the level generator part. The total standing voltage will be further increased when the level count or output voltage needs to be higher. The standing voltage is equal to $((2(3^X-1)-3)+4(2(3^X-1)-3))E$, where X is the number of DC sources. Accordingly, this topology is highly recommended for low-voltage applications, where high voltage levels are required at a low maximum output voltage.

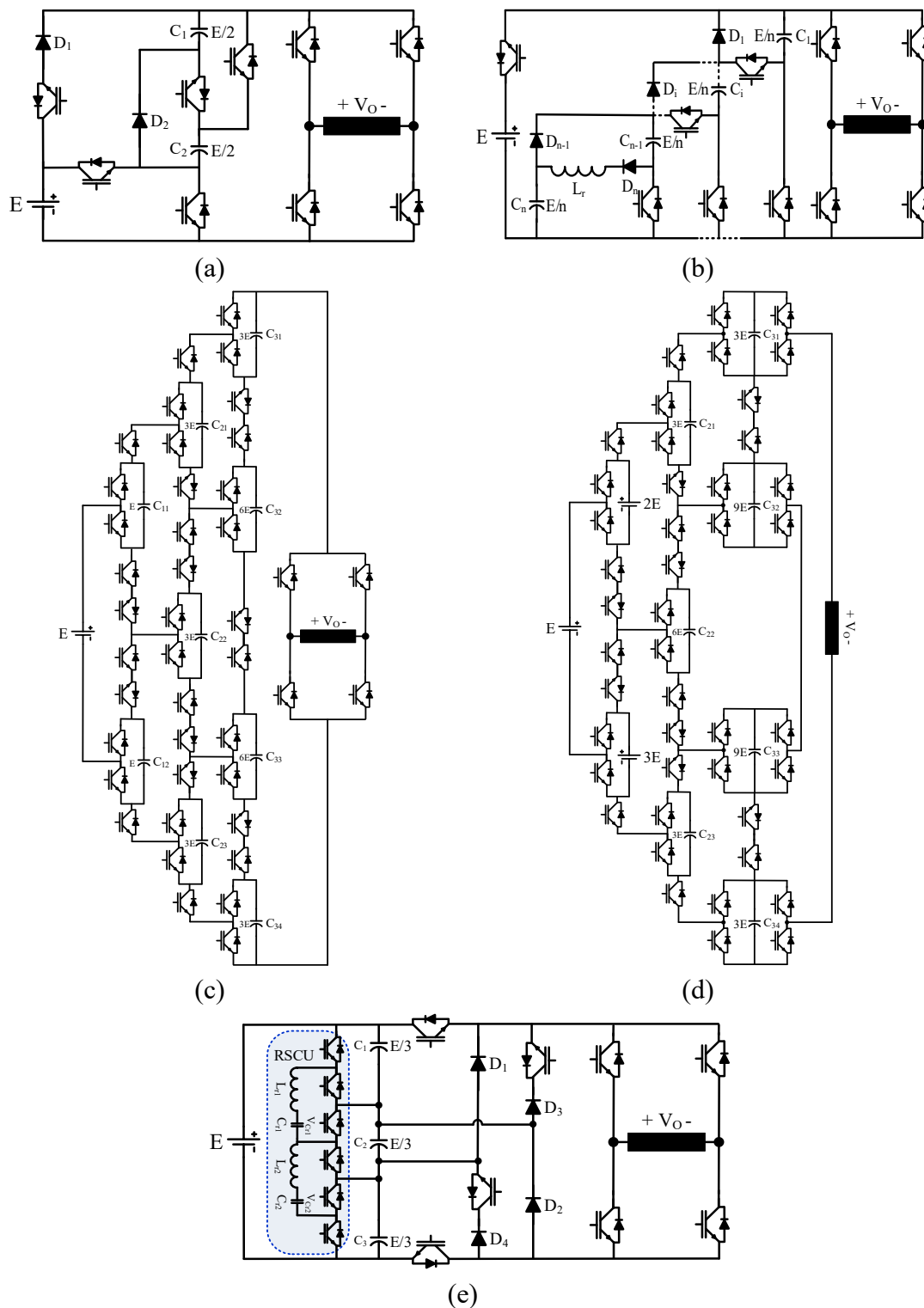


Fig. 8 Unipolar MLI topologies use polarity-changer stage for generating negative voltage levels [55-59]. (a) Nine-level inverter employing one DC source [55]. (b) Quasi-resonant switched-capacitor (QRSC) MLI [56]. (c) Step-up MLI with a single DC source [57]. (d) MLI structure based on a combination of SC and DC sources [58]. (e) Single source seven-level MLI topology [59].

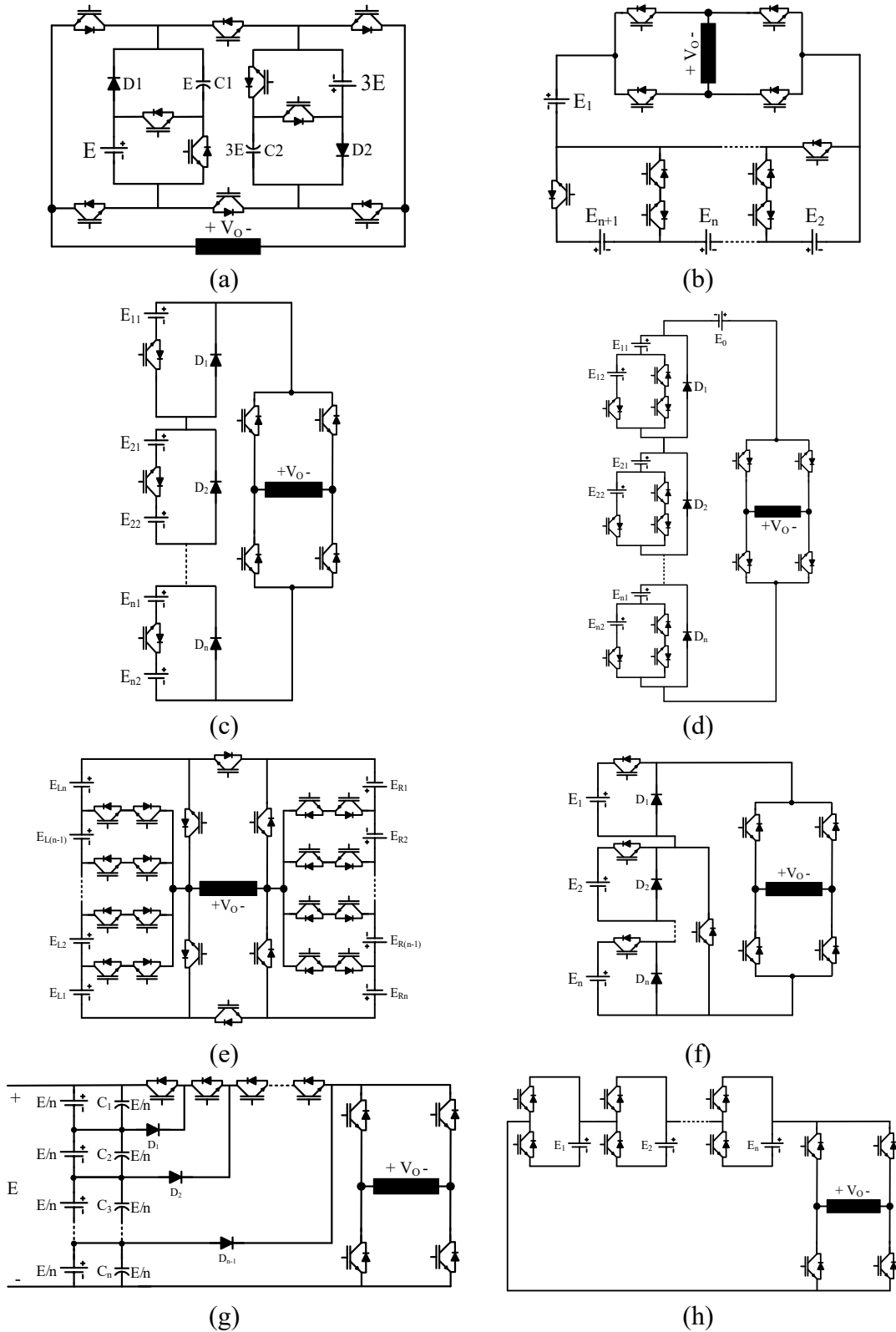


Fig. 9 Unipolar MLI topologies with the polarity-changer stage for generating negative voltage levels [60–67]. (a) 17-level structure for the single-phase SC-MLI [60]. (b) MLI for symmetric and asymmetric structures [61]. (c) MLI topology using single source and double source modules [62]. (d) Symmetric switched diode MLI [63]. (e) Cascaded switch-ladder MLI [64]. (f) Cascaded switched-diode MLI [65]. (g) Switched capacitor-diode MLI [66]. (h) Switched-battery boost-MLI [67].

Unlike the MLIs in [61-67], that use the level generator stage to produce a unipolar multilevel voltage and a polarity changer to obtain bipolar multilevel voltages, resulting in high voltage stresses across the polarity changer switches, the authors in [69] used bipolar units and a full H-bridge cell to construct a novel asymmetrical MLI topology. Fig. 11 (a) shows the generalized configuration of the proposed topology, in which the bipolar units act as a bipolar level generator (BP-LG) while the H-bridge is used to triple the voltage level count of the BP-LG part. For example, to produce fifteen levels, one five-level bipolar unit, which is linked to the H-bridge cell, is required as depicted in Fig. 11 (b). The bipolar unit uses two equal DC sources of $3E$, generating five levels of $6E$, $3E$, 0 , $-3E$, and $-6E$, while the H-bridge uses single DC source of E to generate three levels of E , 0 , and $-E$. Accordingly, fifteen voltage levels can be synthesized. The fifteen-level configuration of the proposed topology requires nine unidirectional switches and four power diodes. The main feature of this topology is its ability for producing high-voltage level count while having structure modularity and using a low number of components and active switches. However, its disadvantages include requiring high counts of DC sources and power diodes when enlarging the voltage levels and the high voltage stresses across the switches of the bipolar unit. For example, in the fifteen-level configuration, S_1 - S_4 have to block voltages of $6E$, and S_5 must block $3E$. When using a second bipolar cell to produce 75 levels, the voltage stresses become $30E$ and $15E$ for the corresponding switches in the second unit. It is worth mentioning that this topology can produce N level either by increasing the number of bipolar cells as in Fig. 11 (a) or/and connecting several modules in cascade (each module has the same structure as the circuit in Fig. 11 (b)). More details for optimized selections of both cell and module counts can be found in [69].

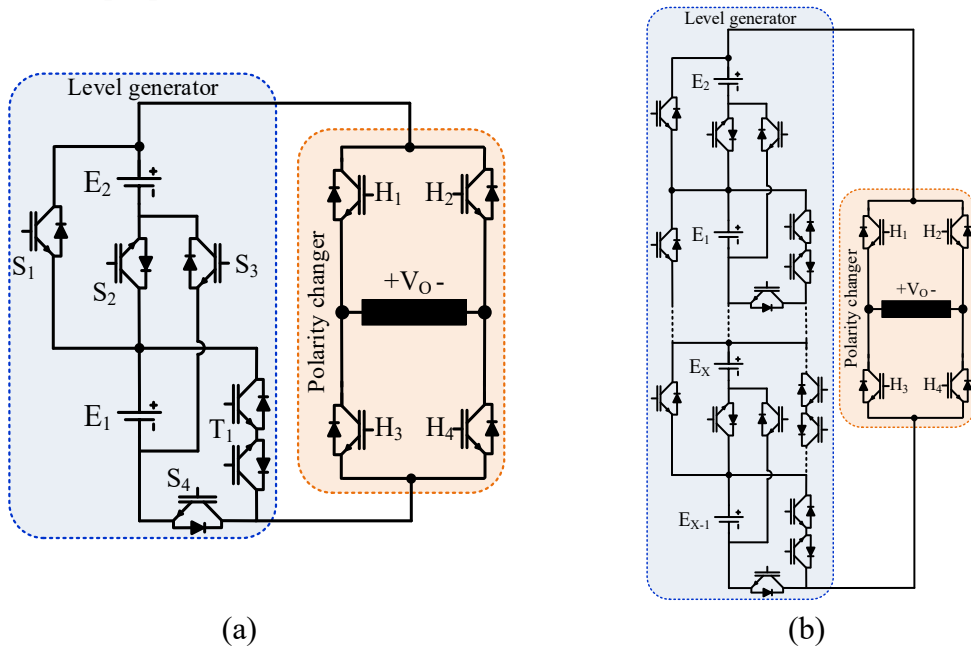


Fig. 10 Asymmetrical MLI with trinary sequence proposed in [68]. (a) Nine-level configuration. (b) Generalized configuration for producing 3^X -level by using X DC sources.

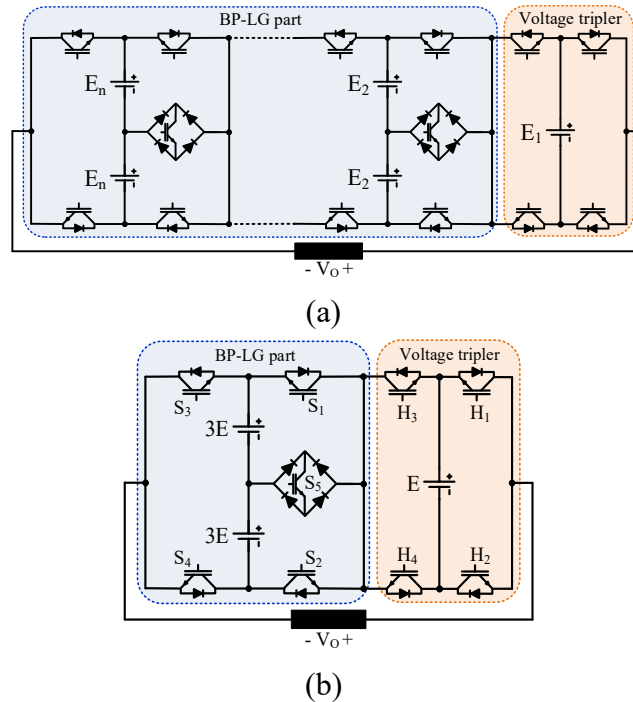


Fig. 11 Asymmetrical MLI topology proposed in [69]. (a) Generalized configuration. (b) Fifteen-level configuration.

A newer single source inverter was proposed in [70], consisting of H-bridges integrated with a bridge-modular-switched-capacitor (BMSC) unit in a way to produce multilevel output with boosting capability. Fig. 12 (a) shows the generalised configuration that uses switched-capacitor (SC) blocks for increasing the voltage level. The boosting capability is a function of the SC blocks number (N_{sc}). The maximum output voltage V_o will be equal to $4 \cdot N_{sc} \cdot E$. For example, using one SC block can produce five levels with the gain of four. Fig. 12 (b) shows the five-level circuit, requiring twelve switches, four capacitors, and one DC source. The traditional CHB MLI uses only eight switches and two isolated DC sources for producing the same levels number with a lower output voltage about 50% (e.g. $E = 50$ V, $V_o = 100$ for CHB, and 200 V for the proposed topology). On the other hand, in the proposed topology, the voltage stress is a function of N_{sc} while in CHB, it is not related to the number of generated levels.

MLIs topologies with the predefined features for specific applications have been designed in [71-75]. The authors in [71] have proposed a new five-level configuration for minimising the leakage current in transformerless photovoltaic (PV) systems. Fig. 13 (a) shows the proposed converter, consisting of two capacitors, eight switches, and two DC sources (to emulate two PV sources) for producing five levels. The basic concept here is to isolate the PVs from the grid during the zero-voltage state by turning off the four switches in H-bridge and using S_a and S_b for forming a new current path. Accordingly, the flow of the leakage current through the parasitic capacitance will be minimized. The switching losses in the switches of the H-bridge will be reduced effectively by enabling a complete turn-off for each half-cycle. On the other hand, the topology in [72] can eliminate the leakage current by connecting the negative terminal of PV to the grid neutral terminal. Therefore, the stray capacitance will be bypassed. Fig. 13 (b) shows the

five-level circuit for the proposed topology in [72]. As compared to the topology in [71], it can eliminate the leakage current in the PV system by using only six switches, three capacitors, and one DC source (to emulate PV source).

For a PV harvesting system, authors in [73] have developed a new seven-level topology for photovoltaic-battery three-input converter applications, including three cascaded H-bridge, one DC source, three capacitors and two switches for charging purpose. The functionality of the proposed circuit can be explained by two operating modes: when the solar energy is available for PVs during the day, the inverter will be used as a three-cascaded H-bridge topology for producing seven levels as shown in Fig. 13 (c). While during the night when the PVs are off, the converter will operate according to Fig. 13 (d), producing seven levels by using only one single source and three capacitors instead of three isolated DC sources (two sources emulate two PV generators) in the first mode.

In some situations, there is a need for connecting two renewable energy sources that generate a different voltage, e.g. PVs and fuel cells (FCs) to load/grid simultaneously by using fewer conversion stages to obtain high efficiency. To address this issue, dual-DC port MLIs (DP-MLIs) was developed in [74], presenting a new five-level DP-MLI. Fig. 13 (e) shows its simplified version based on T-type inverter, consisting of two asymmetrical DC sources, one diode, six switches. As seen in Fig. 13 (e), only one DC port is used for a high-voltage source while the low-voltage source is connected to the lower port. For grid-connected PV applications, the authors in [75] have developed six-switch 5L-ANPC (6S-5L-ANPC) based on the five-level active neutral point clamped inverter (5L-ANPC)

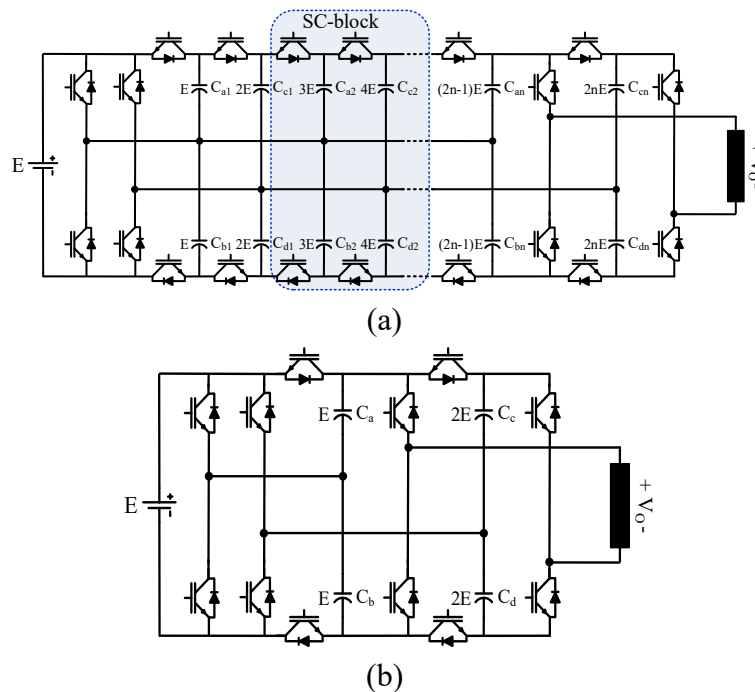


Fig. 12 Flying-capacitor-clamped MLI (FCC-MLI) [70]. (a) Generalised configuration. (b) Five-level configuration.

as shown in Fig. 13 (f). As named, it uses only six switches instead of eight switches like in the traditional 5L-ANPC for producing five levels while requiring two diodes. The idea of reducing the active switches count is based on the fact that

for the grid-connected PV system, the grid voltage and output current are required to be in phase, so it is possible to ignore some paths for reactive current, i.e. some switches can be replaced with diodes.

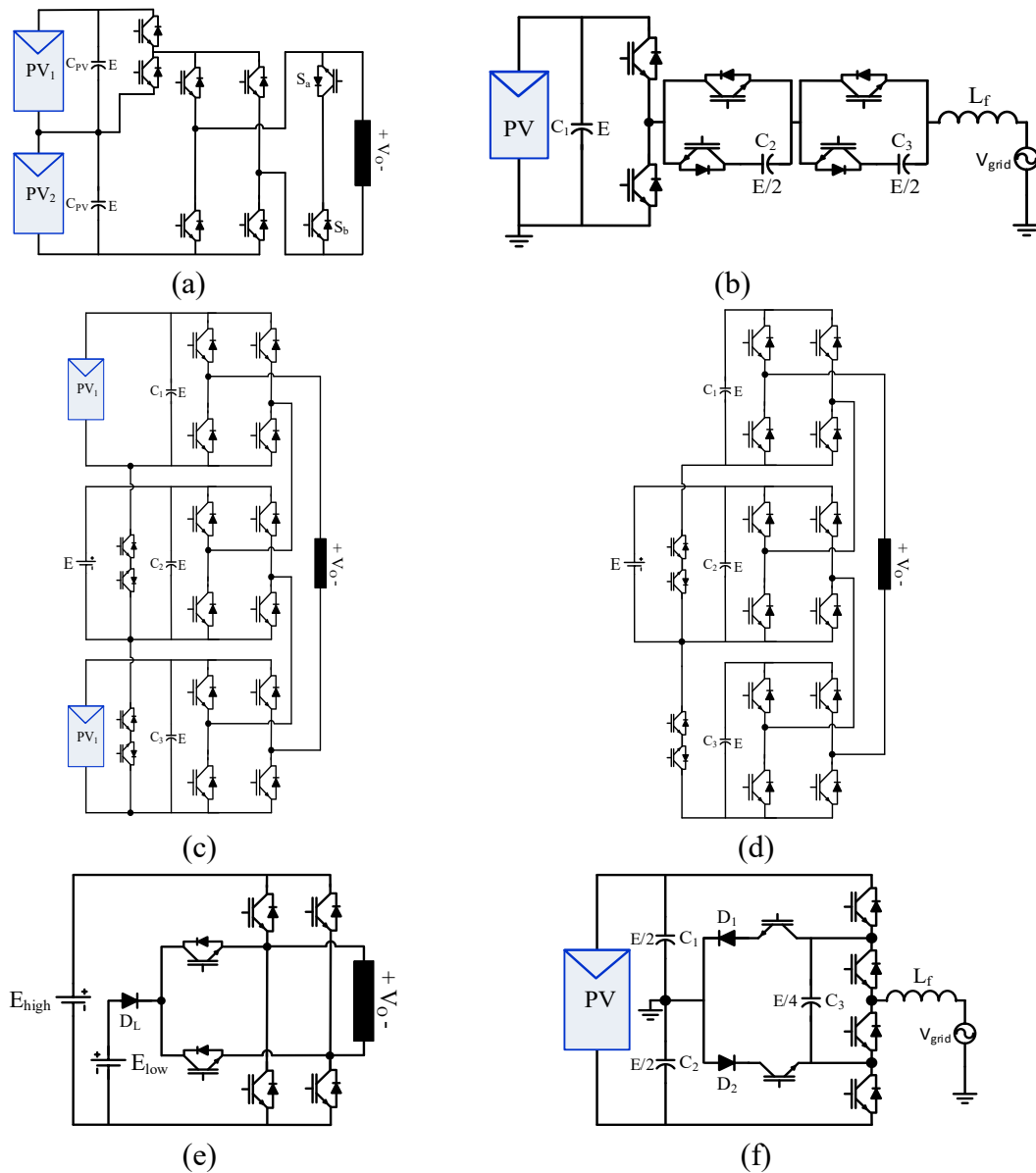


Fig. 13 MLI topologies have predefined features for specific applications [71-75]. (a) Five-level topology for PV systems [71]. (b) Transformerless MLI that eliminates leakage current in the PV system [72]. (c) Seven-level SC topology: when PVs are available during the day [73]. (d) Seven-level SC topology: when PVs are not available during the night [73]. (e) Dual-DC-port asymmetrical MLI [74]. (f) Six-switch five-level topology [75].

A new member of the asymmetrical MLI family was proposed in [76]. This topology has a novel arrangement of components for generating high output levels by using a reduced component count module. Each module needs only ten switches and four asymmetrical DC sources for producing 13 levels. Fig. 14 shows a 25-level configuration, consisting of two primary modules. Although switches have high-voltage stress, especially S_3 and S_4 , the proposed circuit is more applicable in

high-voltage high-power industry because of its modularity feature. Inspired by its shape, it is called as envelope type MLI (E-Type-MLI).

Hybrid MLIs have been an attractive trend in literature. Authors in [77] have presented a hybrid N -level topology using only one DC source. It has three stages: high-voltage stage, connecting-switches stage and low-voltage stage, as seen in Fig. 15. The first and second stages are fixed while the third stage can be repeated for enlarging the voltage level number. Employing one single DC source is one of the main advantages of this configuration while increasing the cost of having a high number of capacitors is a problem. For this reason, the authors have suggested using the second stage to create extra redundant switching states for making the voltage balance of the flying capacitors easier. One repeated stage, e.g. T-type unit-along with the two fixed stages, is needed for producing five levels, requiring ten switches, four capacitors, and one DC source.

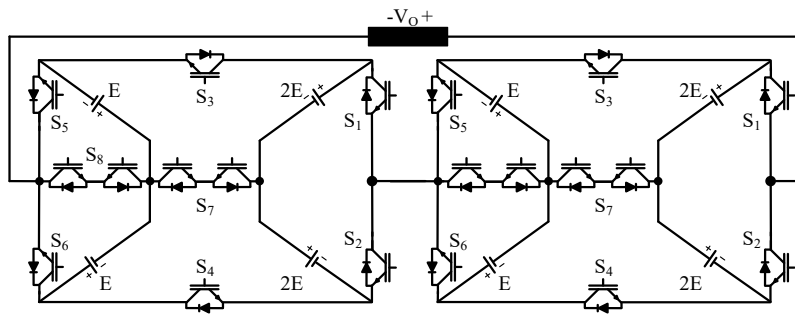


Fig. 14 Envelope type (E-Type) asymmetric MLI [76].

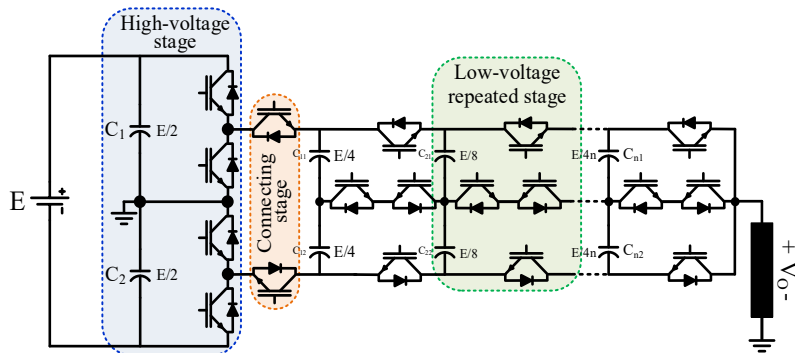


Fig. 15 Hybrid VSI based on T-type topology [77].

A cascaded MLI with a reduced component count was proposed in [78], in which each module has four asymmetrical DC sources. In addition to the four DC sources, it can produce 25 voltage levels with ten switches and eight diodes or can produce only nine-level if using symmetrical DC sources. Connecting modules in cascade results in the N -level configuration of the proposed MLI as shown in Fig. 16. Each module has two 'E' and two '5E' DC sources. The capability of producing negative and positive voltages without using the end-side H-bridge is considered one of the key merits of the proposed MLI. However, high-voltage stress across the switches is the main limitation. For example, the right-hand switches S_1 , S_2 , S_3 , and S_4 have voltage stresses of $2*5E$ while those stresses over the left-side switches S_5 , S_6 , S_7 , and S_8 are $2*E$. Moreover, switches S_R and S_L have voltage stresses of $5E$ and E , respectively. The second asymmetrical N -level topology was presented in [79],

being divided into fixed and repeated stages. The N -level configuration is shown in Fig. 17, in which the fixed stage consists of four switches and two DC sources while the repeated stage comprises two switches and one DC source. Although it uses many asymmetrical DC sources for increasing the levels number, it does not use diodes and capacitors, being more attractive features. For generating 15 levels, it requires only eight switches, and three DC sources with a magnitude of E , $2E$ and $5E$. It is worth mentioning that the voltage stress of the switches is a function of levels number. For example, producing 15-level requires four pairs of switches withstand for voltage stresses of $2E$, $7E$, E , and $4E$, fitting well for low-voltage applications.

A group of cross-switched topologies was introduced in [80-82]. Connecting two T-type legs back-to-back was presented in [80], resulting in a new cross-switched T-type based MLI. It uses two cross-connected switches to connect two identical T-type modules in a back-to-back manner, as illustrated in Fig. 18 (a). The cross-switched T-type MLI requires six unidirectional switches (S_1 - S_6), two bidirectional switches (T_1 and T_2), and four DC voltage sources (E_1 - E_4) to produce nine voltage levels of $-4E$, $-3E$, $-2E$, $-E$, 0 , E , $2E$, $3E$, and $4E$ when using symmetrical DC sources ($E_1 = E_2 = E_3 = E_4 = E$), while seventeen voltage levels can be synthesized for the asymmetric operation ($E_1 = E_2 = E$, and $E_3 = E_4 = 3E$). The high voltage stress across the six unidirectional switches is considered as the main disadvantage of this topology. For example, in the symmetrical operation, the voltage stress across switches S_1 - S_4 is $2E$, while it is equal to $4E$ for both S_5 and S_6 . The situation becomes worse for the asymmetrical mode of operation, where the voltage stress is $2E$, $6E$, and $8E$ for switches (S_1 and S_2), (S_3 and S_4), and (S_5 and S_6) respectively. Low component count, being capacitor-, inductor free, and generating negative voltage levels without using H-bridge are its advantageous features. Another merit of this circuit is the extension possibility. The level count can be enlarged to N levels by cascading the configuration in Fig. 18 (a), as recommended by the authors in [80] and shown in Fig. 18 (b). For producing N levels, $(1.25N-1.25)$ switches and $(0.5N-0.5)$ DC sources are required for the symmetrical operation, while under the asymmetrical mode, these numbers become $5(N-1)/8$ switches and $(0.25N-0.25)$ DC sources.

Unlike the cross-switched topology in [80], where only T-type modules are integrated with two cross-connected switches, the authors in [81] use the T-type module accompanied with two new modules for forming a single-source step-up MLI topology. Fig. 19 shows its generalized configuration, consisting of three structures: T-type module, cross-connected module, and input module. Among these three modules, only the cross-connected module can be repeated to configure an extendable structure. The N -level voltage requires $(N-1)/2$ capacitors, $((1.5N-1.5)+5)$ switches, and $(0.5N-2.5)$ diodes. For example, for building a thirteen-level configuration, six capacitors, twenty-three switches, and four diodes are required in addition to one DC source. The proposed topology can step up the input voltage (E) to reach a required value by using several capacitors, acting as floating power supplies. Each capacitor is charged to E , boosting the input voltage by a gain of $(N-1)/2$. However, this feature results in a problem of increasing the number of capacitors, or size and control complexity. Further, the current spikes, that are

common in several switched capacitor topologies [81], need to be reduced by some strategies as detailed in [81]. On the other side, the proposed topology has some of the remarkable merits, like producing higher counts of voltage level without increasing the voltage rating of switches (voltage stress does not exceed $4E$) and generating bipolar voltage waveforms without the need of an H-bridge.

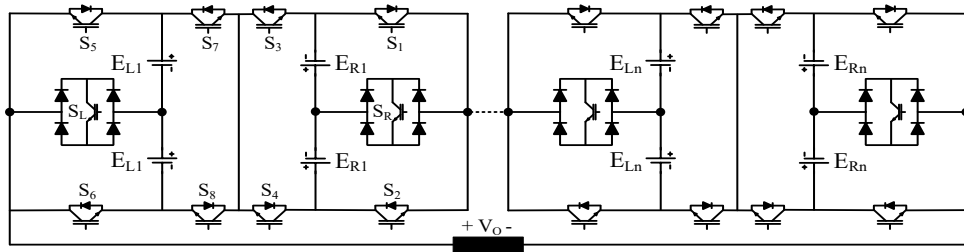


Fig. 16 Cascaded MLI based on a new module with symmetric or asymmetric DC sources [78].

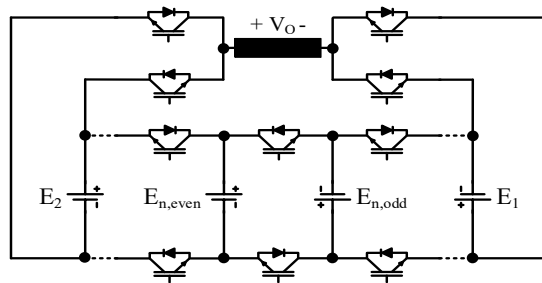
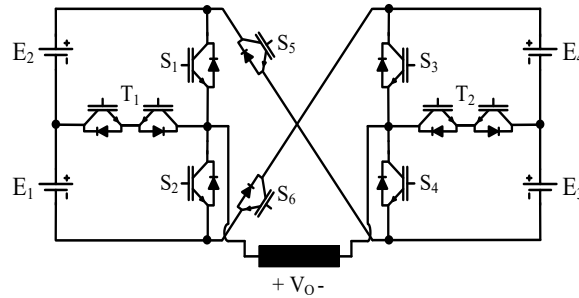
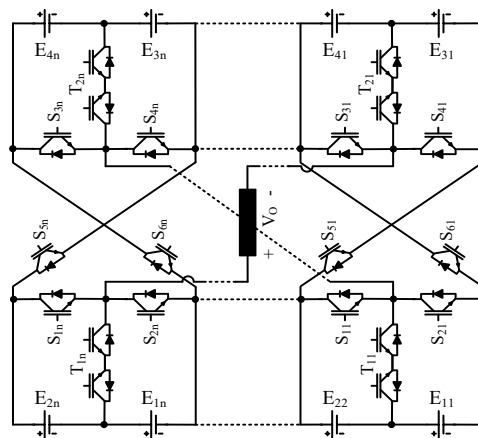


Fig. 17 Asymmetrical MLI with a reduced number of switches [79].



(a)



(b)

Fig. 18 Cross-switched T-type MLI [80]. (a) Nine-, seventeen-level configuration. (b) Generalized configuration.

Another member of the cross-switched MLIs was presented in [82]. It is a cascaded cross-switched topology that can be configured with symmetric or asymmetric DC sources for producing a high-resolution output voltage. Fig. 20 (a) shows its N -level configuration, consisting of cascaded M modules. Each module is structured by using K basic cells in cascade. The output level count can be enlarged by increasing the number of either module or basic cells, or both of them. For example, $(2MK+1)$ and $(4K-1)^M$ voltage levels can be obtained from symmetrical and asymmetrical DC sources, respectively, if using (MK) DC sources and $(2MK+2M)$ switches. The authors in [82] recommended a configuration as shown in Fig. 20 (b), being constructed by using two modules, where each has two basic cells (i.e. $M=2$ and $K=2$). It requires twelve switches and four DC sources for producing 9 and 49 levels for symmetrical and asymmetrical operations, respectively. Besides features of being capacitor- and inductor free, the modularity is considered its main merit, allowing for producing N -levels without increasing the total standing voltage of the switches. Having a low standing voltage of switches requires many isolated DC sources, making this topology more applicable to PV systems.

A boost active-neutral-point-clamped MLI (ANPC-MLI) was recently proposed in [83], which was derived from an improved five-level ANPC topology in [84]. As compared to the topology in [84], the topology in [83] improves both the voltage gain and level count. The voltage gain can be improved from 1 to either 1.5 or 2.5 while the level count is increased to seven, nine, and eleven levels. These positive features must be compensated by an increase of the switch and flying capacitor counts. Fig. 21 shows both structures of the proposed topology in [83], in which the structure A can generate seven voltage levels with a voltage gain of 1.5, requiring only one extra switch as compared to the five-level ANPC topology in [84]. The structure B can produce nine and eleven voltage levels with the voltage gains of unity and 2.5, respectively, increasing one flying capacitor and three switches as compared to the topology in [84]. The level count in the structure B has two values (nine or eleven) based on the charged voltage of the two flying capacitors C_3 and C_4 . When being charged to $0.25E$, the obtained level count is nine. The level count becomes eleven when being charged to E . It is worth mentioning that the voltage stress across switches cannot exceed E for generating seven and nine voltage levels. The voltage stress does not exceed $2E$ for producing eleven voltage levels.

To combine the merits of quasi-Z-source (qZS) and multilevel inverters, the concept of qZS was applied to MLI topologies [85-87], resulting in a family of buck-boost single-stage MLIs with the shoot-through withstanding capability. The authors in [85] proposed a new qZS multilevel topology based on the diode-clamped five-level inverter as depicted in Fig. 22. Two identical qZS networks are used for boosting the input voltage of a single DC source by a factor of B_f , where B_f is equal to E'/E_{in} and called boost factor. Then the five voltage levels of $-B_f E$, $-0.5B_f E$, 0 , $0.5B_f E$, and $B_f E$ are generated by the diode-clamped structure. Fig. 22 shows the proposed circuit, producing five voltage levels when using eight switches, six diodes, four inductors, four capacitors, and a single DC source. It is noted that the presented configuration in Fig. 22 can be extended to a three-level

three-phase qZS inverter by adding one more inverter leg (four switches and two diodes) [85]. Using low-rated switches, single DC source, and continuous input current are the advantageous features of the proposed topology. On the other hand, increasing the number of diodes in the circuit and having a boost factor similar to the classic qZS inverter are considered as its main shortcomings [86]. A novel quasi-Z-source (qZS) topology was proposed in [86], integrating a modified impedance network with the MLI topology introduced in [88]. Fig. 23 (a) shows its five-level configuration, in which four capacitors, two inductors, and three diodes are used for constructing the modified impedance network while six switches are used for producing multilevel output. The proposed topology requires a lower component count as compared to the five-level qZS-MLIs in [85, 87], reducing the inductor count by 50% while keeping the same count of switches and

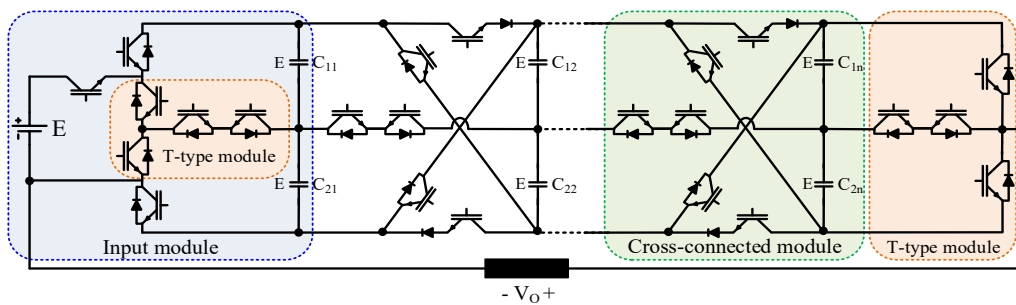


Fig. 19 Generalized configuration of the step-up topology in [81].

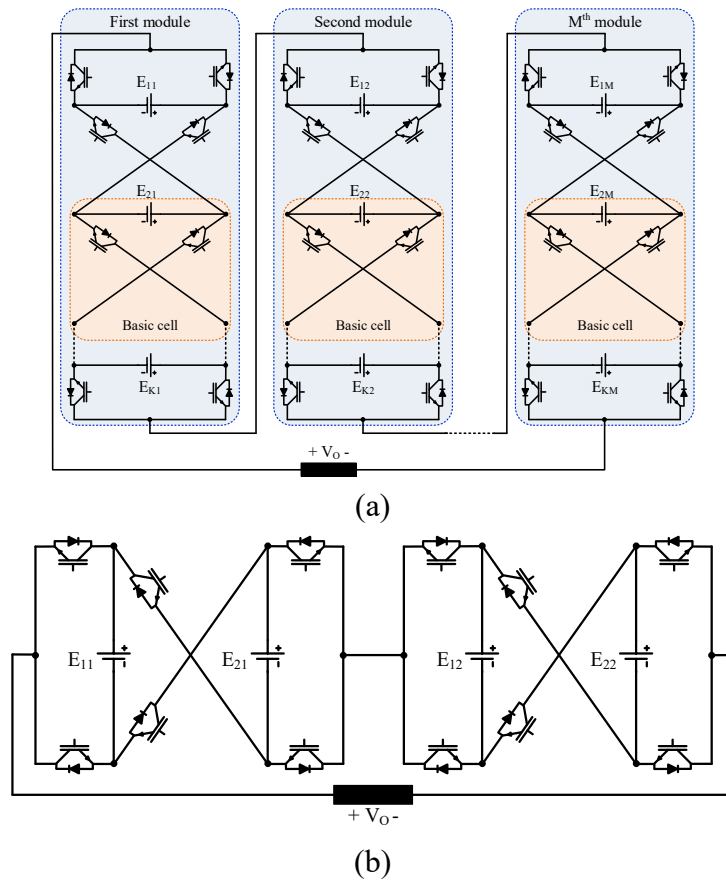


Fig. 20 Cascaded cross-switched topology in [82]. (a) Generalized configuration. (b) Nine-, 49-level configuration.

capacitors. As compared to the topology in [87], it saves one DC source, but requires one extra diode. When comparing with the circuit in [85], it reduces the diode count by three diodes. Further, the proposed topology can double the boost factor, which is not possible in [85, 87]. To achieve these remarkable features, the current stresses of inductors (L_1 and L_2) and the voltage stresses of four switches (H_1 - H_4) are doubled. It is worth mentioning that the switches H_1 - H_4 are necessary for producing bipolar voltage waveforms and have a rating of full dc-link voltage. Their voltage stress also rises when enlarging the level count. For example, Fig. 23 (b) shows the nine-level configuration of the proposed topology, in which two five-configurations are cascaded, doubling the voltage stresses across switches the H_1 - H_4 .

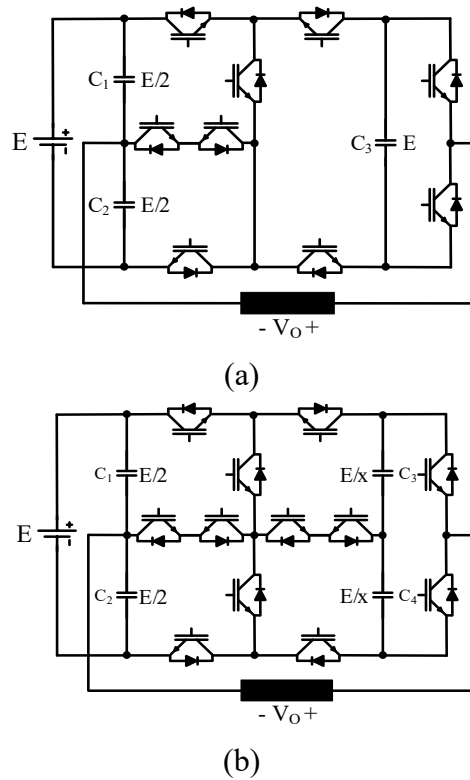


Fig. 21 Boost active-neutral-point-clamped MLI (ANPC-MLI) proposed in [83]. (a) Structure A, seven-level boost ANPC. (b) Structure B, nine-level ($X=4$) or eleven-level ($X=1$) boost ANPC.

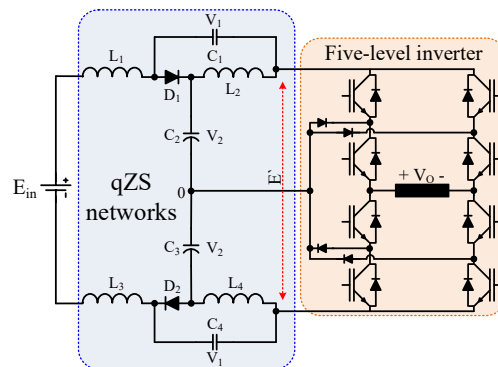


Fig. 22 Five-level quasi-Z-source inverter proposed in [85]. $V_1 = DE_{in}/(2 - 4D)$, $V_2 = (E_{in}(1 - D))/(2 - 4D)$, where D is the shoot-through duty cycle.

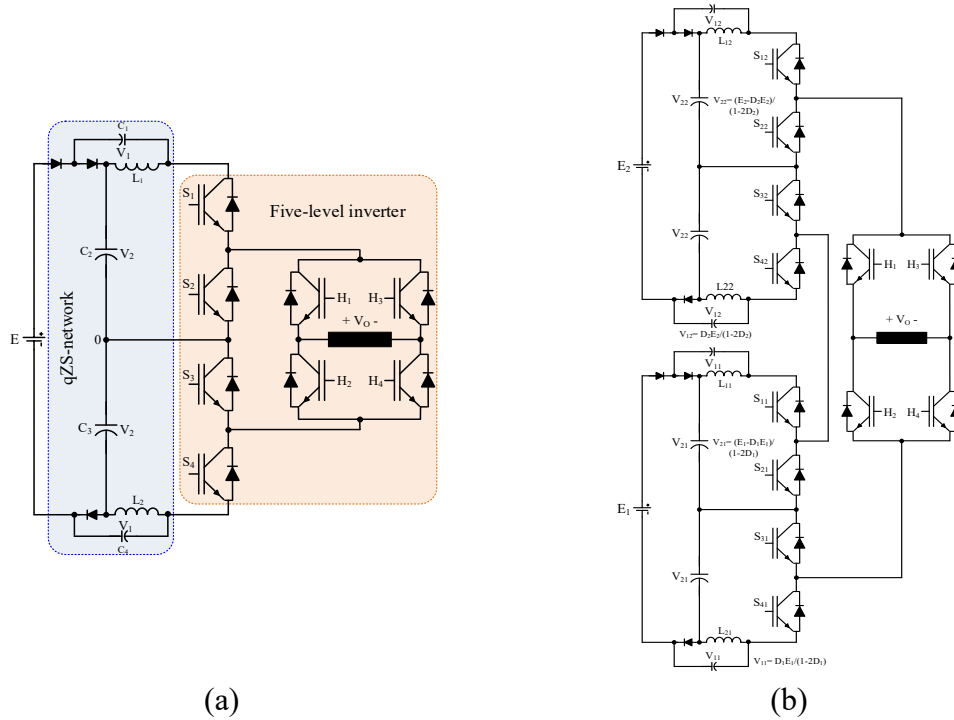


Fig. 23 Modified qZS multilevel inverter in [86]. $V_1 = DE/(1 - 2D)$, $V_2 = (E - DE)/(1 - 2D)$, where D is the shoot-through duty cycle. (a) Five-level configuration. (b) Nine-level configuration.

B. THREE-PHASE MULTILEVEL INVERTERS

This section presents a review of the recently proposed three-phase MLIs based on their operation, advantages, and disadvantages, making the selection of suitable applications easier. The reported topologies in this section represent different types of MLIs such as single source, inductor-based, symmetrical, asymmetrical MLIs for hybrid and non-hybrid configurations. Further some topologies for improving the power quality of power system are included.

One of the salient members in the neutral-point clamped MLIs family is the T-type inverter. It is also known as a neutral-point-piloted inverter (NPPI) and considered as one of the most popular three-level topologies [89, 90]. A single-phase T-type inverter was patented by Conergy in [91], and the authors in [92] presented the three-phase T-type configuration. Fig. 24 shows the T-type inverter for three-phase applications, consisting of a conventional two-level VSI combined with three branches of bidirectional switches, being assumed as a common-emitter configuration. Each branch connects the midpoint of the DC link to one leg of the two-level VSI, forming a T-type shape. The six switches of the VSI (S_1 - S_6) are rated at the input voltage E , while the remaining switches have voltage ratings of $0.5E$. One counterpart to the T-type MLI is the diode-clamped MLI, which requires six clamping diodes while the T-type uses six switches instead. Both of them uses a single DC source and two capacitors, and twelve switches for producing three voltage levels. The distinct feature of the diode-clamped inverter is that it has lower voltage stresses of the switches ($0.5E$) than those in the T-type (six switches of E , six switches of $0.5E$), reducing the switching losses. On the other hand, the T-type inverter has a lower component count in the current path, reducing the conduction

losses. Further, only one switch is required in the current path for positive or negative output voltage while two switches are needed in the diode-clamped inverter regardless of the output level [90-94]. Accordingly, the T-type MLI is more advantageous in applications, requiring low switching frequencies alone.

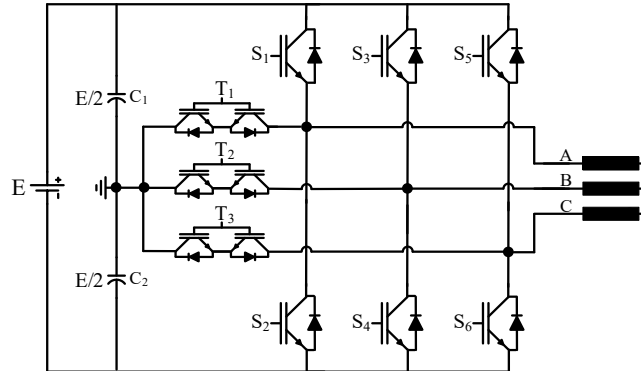


Fig. 24 Three-phase T-type multilevel inverter [92-94].

Single-stage multilevel inverters (SS-MLIs) with boosting capability have been recently proposed in [95-97] for PV, uninterruptible power supplies (UPS), and fuel cells (FCs) applications. Typically, the boosting stage and multilevel stage are merged to form single-stage converters that have both merits of boost converters and MLIs. For example, a new SS-MLI called three-level LC-switching based NPC (3L-LC-NPC), was presented in [95]. Fig. 25 (a) shows its complete configuration, consisting of a boosting circuit (BC) connected to a conventional three-level NPC, allowing for the capability for boosting the input voltage and producing improved quality output. The BC consists of four diodes, two switches, two inductors, and two capacitors, while twelve switches, six diodes, and two DC sources are required for the three-level NPC circuit. Compared to the conventional Z-source MLIs (ZS-MLIs) in [98, 99], the proposed topology reduces 50% of capacitor and inductor count, and having a continuous input current, but uses two extra diodes and two switches. In addition to the NPC limitations, using several high-power passive elements in the boosting stage increases the weight, cost, complexity, and the losses of the inverter.

Another topology of SS-MLIs with the boosting feature was introduced in [96], producing the same voltage levels like the topology in [95]. Instead of using NPC, the topology in [94] uses a T-type MLI to produce multilevel waveforms. Two identical quasi-Z-source networks are used for the boosting circuit, as shown in Fig. 25 (b). Compared to the topology in Fig. 25 (a), only two diodes are required by using the T-type MLI. Without using switches in the BC, the count of capacitors and inductors is doubled. Three bidirectional switches in the topology increase the redundancy of the switching states, enabling fault-tolerant capabilities for some common faults, e.g. open-circuit failures. Fig. 25 (c) shows a new three-level topology proposed in [97], having the same number of the levels in [95, 96]. This topology is an upgraded configuration of the two-level split-source inverter (SSI) in [100]. Because of its ability for generating a boosted voltage with three-level waveforms, the direct connection of low-voltage energy sources, namely PVs and

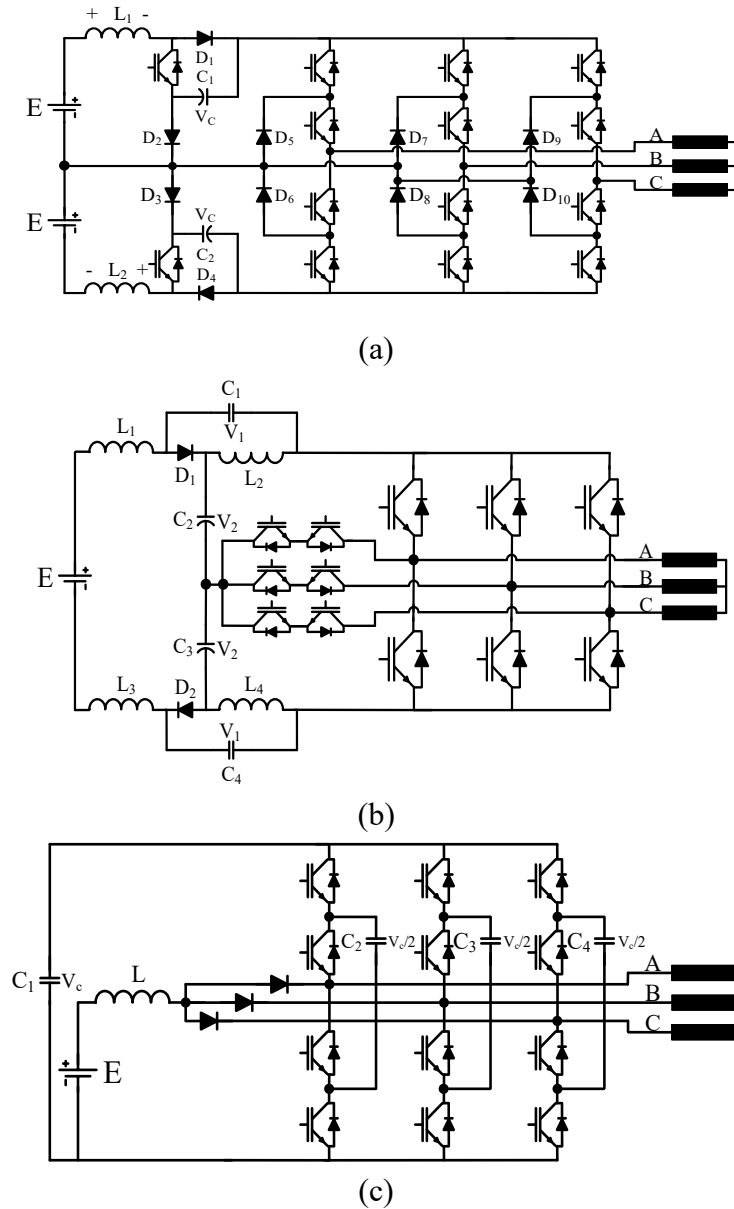


Fig. 25 Single-stage multilevel inverters with boosting capability [95-97]. (a) Three-level LC-switching-based voltage boost NPC MLI [95]. $V_c = E/(1 - 2D)$, where D is the shoot-through duty cycle. (b) Quasi-Z-source inverter with a T-type MLI [96]. $V_1 = DE/(2 - 4D)$, $V_2 = (E(1 - D))/(2 - 4D)$, where D is the shoot-through duty cycle. (c) Three-phase three-level flying capacitors split-source MLI [97]. To maintain a three-level operation, V_c should be larger than $2E$.

fuel cells, become more accessible and efficient. Producing three levels needs twelve switches, three diodes, four capacitors, one inductor, and one DC source. The proposed topology has several attractive features like boosting capability, using a single DC source, continuous input current, and having a reasonable number of passive components. On the other hand, several limitations can be found as high-current and -voltage stresses on the used semiconductor devices, lack of modularity, increasing the control complexity and system footprint, decreasing the expected lifetime because of using flying capacitors and inductor. Further, this topology needs extra efforts in control algorithms for removing the low-frequency

in [105]. As observed in Fig. 28, using a significant number of flying capacitors and diodes, along with lack of modularity are the main limitations of this circuit. However, using less DC sources and having low-voltage stress across the switches are its main features. In [104], the authors have proposed a new six-level topology, being formed by combining three three-level flying capacitor legs with six two-level legs as shown in Fig. 29. Despite using only one DC source, six capacitors and 24 switches are required for producing a three-phase voltage. While having a reduced count of switches and DC sources, the proposed inverter must use many capacitors that have diversified voltage ratings, requiring a voltage control for the flying and DC-link capacitors. Therefore, the authors have used the reported circuit in [106] for balancing the capacitors in the DC-link, along with a pre-charging process for the flying capacitors. For the proposed topology, it is important to mention that the auxiliary circuit for voltage balance of the DC-link capacitors is especially essential at a wide range of load power factor (PF) [104].

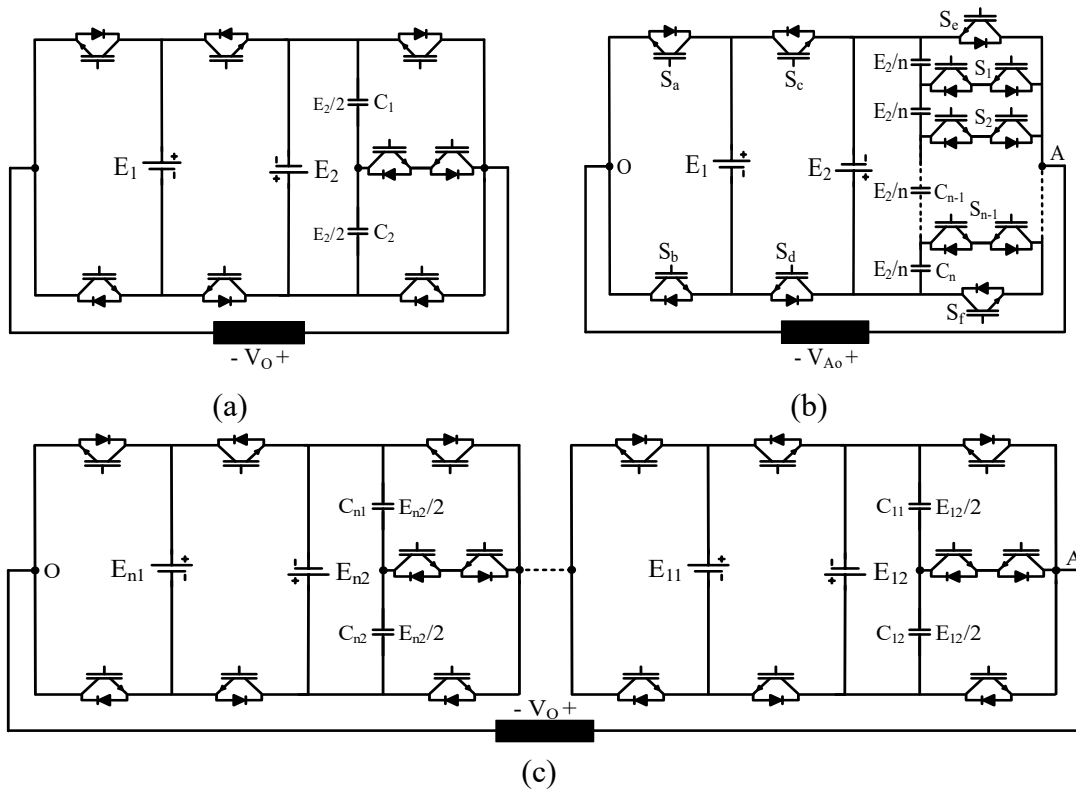


Fig. 27 MLI for interfacing renewable energy sources with low-, medium- and high-voltage grids [102]. (a) Basic unit for generating 7-, 9-, and 11-level. (b) Two DC sources N -level configuration (leg A). (c) Multiple DC sources N -level configuration (leg A).

In transformerless PV systems, designing converters requires features like boosting capability, longer lifetime and zero common-mode voltage (CMV) [107]. To design a zero CMV converter, a modified T-type three-level inverter was presented in [107], merging the traditional T-type inverter with a DC-link that has four capacitors through two pairs of switches as shown in Fig. 30. Contrary to other solutions for eliminating the CMV in [108], the proposed topology has a low count of switches and capacitors and uses only 16 switches and four capacitors while eight capacitors and 24 switches are required in [108]. However, the total standing

voltage of the switches in [107] is higher than that in [108]. Further, for PV systems connected to a microgrid, a new hybrid modular multilevel inverter (MMLI) was proposed in [109]. Because of using a high number of DC sources, it is most applicable for PV farms where realising DC voltage is easy. Fig. 31 shows the schematic diagram of its three-phase arrangement, in which a three-level T-type inverter works as the main stage, and a new four-level cell is connected in cascade for producing more levels. The new four-level cell is a modified full H-bridge and constructed from two capacitors, four switches and two DC sources. The reduced switch count and the ability for operating in symmetrical or asymmetrical modes are the main features of this MLI. By employing the asymmetrical mode, the output level number will be increased while the component count will be the same. However, the topology must use different DC sources with proper voltage ratings, increasing the voltage stress across some switches. By using only one cell per phase in addition to the main stage, nine voltage levels can be achieved with 24 switches, eight capacitors, and seven symmetrical DC sources.

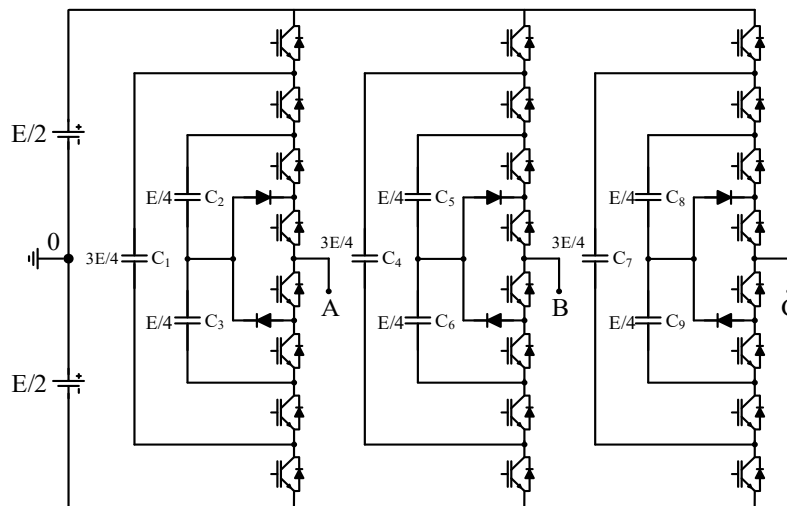


Fig. 28 Five-level VSI for medium-voltage applications [103].

A new optimised multilevel topology was presented in [110], and Fig. 32 shows its configuration for producing N levels. Despite using the same main stage as topology in [109], i.e. T-type MLI, it has a different level-generator (LG) stage for enlarging the level number. Further, it is noted from Fig. 32 that the LG stage is subdivided into two identical units of one DC source and N_{HBs} half H-bridge cells. This topology could work as a symmetrical and asymmetrical MLI, requiring $(4N_{\text{HBs}} + 12)$ switches and $(2N_{\text{HBs}} + 2)$ DC sources for producing $(N_{\text{HBs}} + 3)$ and $(2^{N_{\text{HBs}}} + 2)$ levels for symmetrical and asymmetrical operation, respectively. Diode-, capacitor-, inductor-free and low component count are the main features of this circuit. In contrast, lack of modularity is considered the main demerit of this inverter, limiting the level count because of high-voltage stress across the six unidirectional switches in T-type stage. These switches must withstand a voltage equal to the generated voltage by the LG stage.

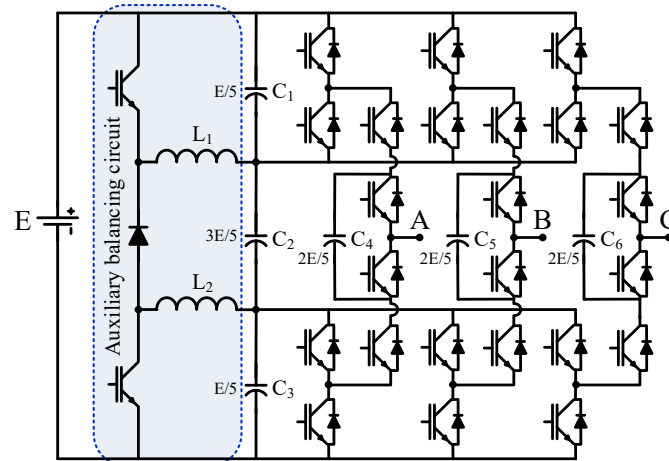


Fig. 29 Six-level MLI topology for medium-voltage applications [104].

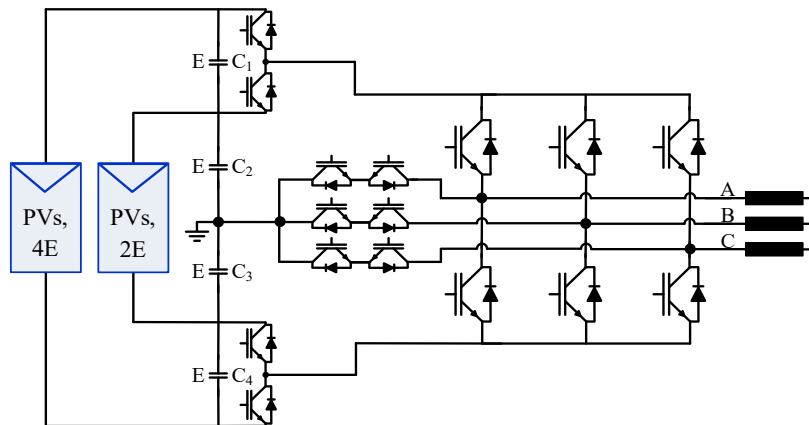


Fig. 30 Modified T-type three-level inverter for minimising CMV [107].

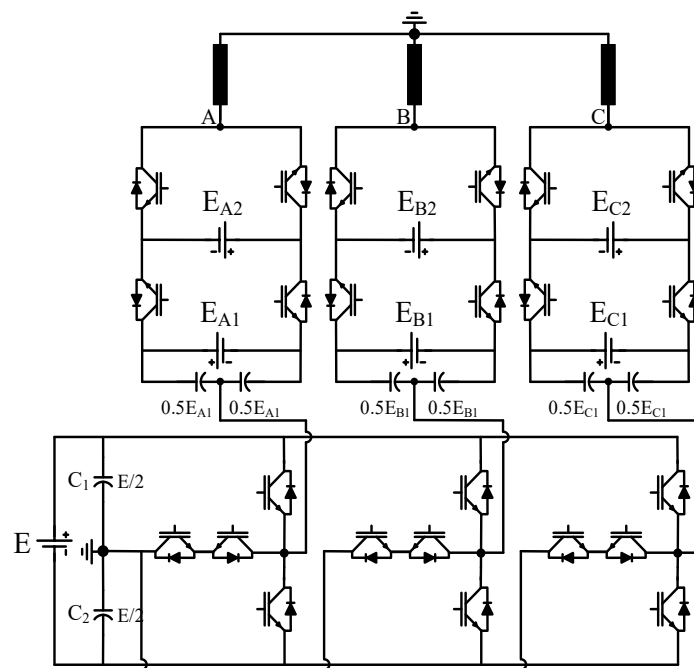


Fig. 31 Three-phase hybrid MLI for renewable energy [109].

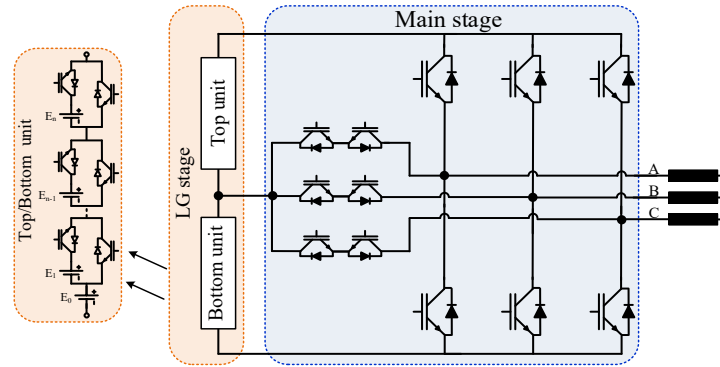


Fig. 32 Three-phase MLI topology with separate level and phase sequence generation part [110].

Novel asymmetrical hybrid inverters in [111, 112] can produce N levels with a reduced component count. The topology in [111] has two different stages, as shown in Fig. 33. Stage I consists of a traditional six-switch two-level inverter connected to DC-link through a bidirectional switch network, in which each DC source is connected through one switch to one inverter leg. Stage II consists of three half H-bridge cells (one cell for each phase). Stage II is responsible for doubling the level count, so it is called a doubling unit. In spite of reducing the component count, it increases the rating voltage of components. As seen in Fig. 33, by using N_{DC} voltage sources of E , six switches must withstand $N_{DC} * E$, and the other six switches in stage II have a rating more than $N_{DC} * E$ and different ratings of the bidirectional switches based on its position. Alternatively, Fig. 34 shows the non-isolated-source based topology reported in [112], using stage II of topology in [111] to build a string of cascaded cells that are responsible for producing $(N-2)$ levels. Moreover, two extra levels are generated by a new structured unit (NSU). As shown in Fig. 34, the NSU is formed by three modified cells connected in

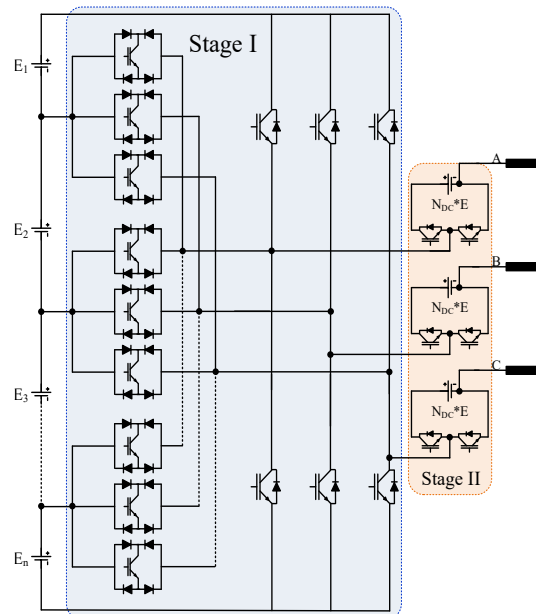


Fig. 33 Three-phase MLI using voltage doubling-unit [111].

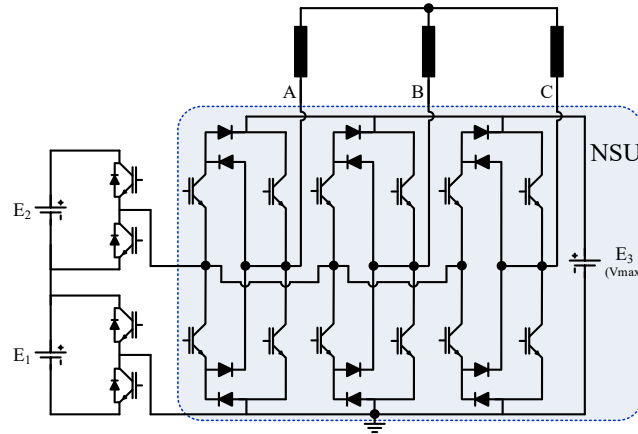


Fig. 34 Three-phase configuration based on cascaded half-bridge [112].

parallel with a DC source of V_{\max} . The NSU can produce minimum and maximum levels of the generated voltage, i.e. 0 and V_{\max} , while the half H-bridge string generates the rest of levels. Generating four levels requires three DC sources of E , E , and $3E$ besides sixteen switches and twelve diodes. Although the number of levels is maximized in term of the component count, the total standing voltage is dramatically increased in a similar way to the topology in [111].

The concept of generating a high number of levels by stacking capacitor-based full H-bridge cells was used in [113]. This concept is widely adopted for designing new circuits by using a low number of DC sources while increasing the number of flying capacitors. For enlarging the number of levels, each group of the capacitors has a different voltage reference as compared to previous and subsequent groups. Therefore, additional voltage balancing algorithms are required for maintaining the capacitor voltages at the respective values. The nine-level circuit for the topology in [113] is depicted in Fig. 35, in which each phase has two three-level FCs, one selector cell, and one capacitor-fed full H-bridge unit (CF-HB). Producing nine levels requires two symmetrical DC sources (each of $0.5E$ volt), 42 switches (6, 24, and 12 switches having blocking voltages of $0.5E$, $0.25E$, and $0.125E$, respectively), and nine capacitors (six of $0.25E$ and three of $0.125E$). It can generate N levels by increasing the number of FC and CF-FB cells, in addition to a modification in the selector cell.

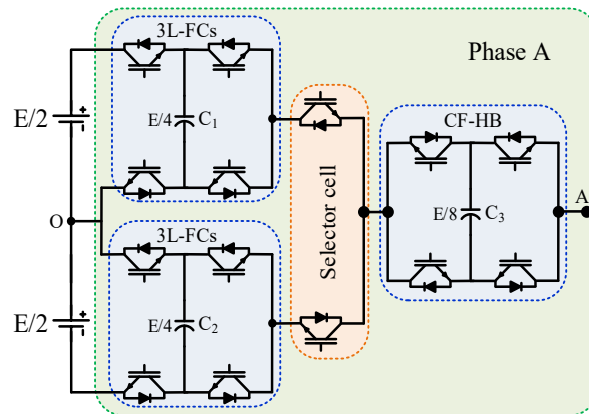


Fig. 35 One phase of a topology formed by stacking inverters of lower multilevel structures [113].

Based on the conventional two-level voltage source inverter (2L-VSI), two MLIs were proposed in [114, 115]. In [114], the authors have presented a novel arrangement of two 2L-VSI. The proposed topology can generate N levels by using N_{DC} voltage sources and $(2(N_{DC})^2 + 2N_{DC})$ bidirectional switches, where each switch is built by connecting two unidirectional switches in the common-emitter configuration, reducing the required gate driver count. Fig. 36 shows its scaled-down circuit, being formed by connecting only two 2-level inverters in parallel while requiring 24 switches and two asymmetrical DC sources of E_1 and E_2 volt. Under the suggested PWM scheme by the authors, it can provide four levels $-E_1$, 0 , E_2 , and (E_1+E_2) in the pole voltage and six-level line voltage. Using a high number of switches is one key limitation of this topology while using a low number of DC sources and having low requirements for the gate driver circuits are the main features. Contrary to connecting the 2L-VSIs as in [114], the authors in [115] have merged them in a distinct way for constructing a novel three-level unit as depicted in Fig. 37, in which two symmetrical DC sources and only twelve unidirectional switches are used. Several units with extra three switches must be cascaded for enlarging the number of levels. This topology has merits of using a low count of DC sources, and capacitor- and diode-free, being beneficial for control simplicity, compact design, long lifetime and low cost. However, a moderate total standing voltage of the bottom three switches S_4 , S_8 , and S_{12} is the main limitation of this MLI.

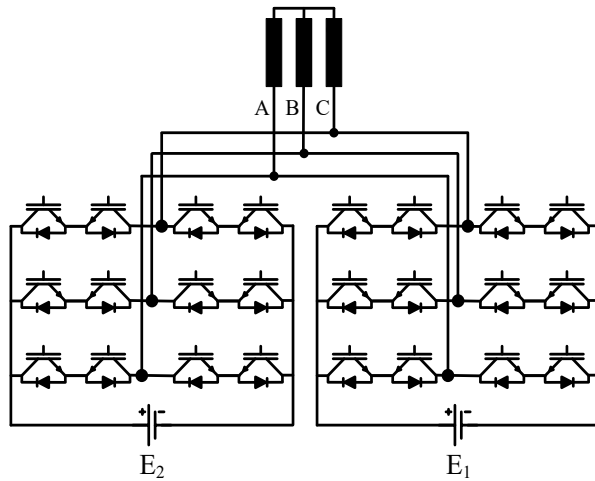


Fig. 36 Four-level topology for renewable energy grid integration [114].

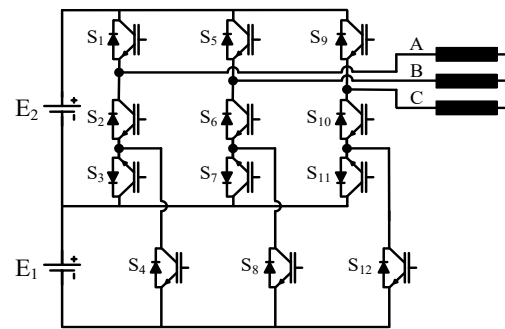


Fig. 37 Three-phase three-level MLI based on two-level VSI [115].

A three-phase single source topology for standalone applications was presented in [116]. It is formed by three identical legs, sharing the same DC-link. Each leg has two unidirectional switches and two bidirectional switches, as shown in Fig. 38. The DC-link consists of a single DC source accompanied by three voltage-divider capacitors C_1 , C_2 , and C_3 . Controlling switches in each leg properly allows this topology to produce four levels 0 , $E/3$, $2E/3$, and E in the pole voltage V_{A0} , or result in seven levels of E , $2E/3$, $E/3$, 0 , $-E/3$, $-2E/3$, and $-E$ in the line voltages. Using a single DC source, low count of active switches, and having only three ON-switch at any level are its main advantages. Its key disadvantages include using three capacitors, twenty-four power diodes, and high-voltage stresses, which are

equal to the full dc-link voltage across the six unidirectional switches while the six bidirectional switches must block 66.67% of the full dc-link voltage.

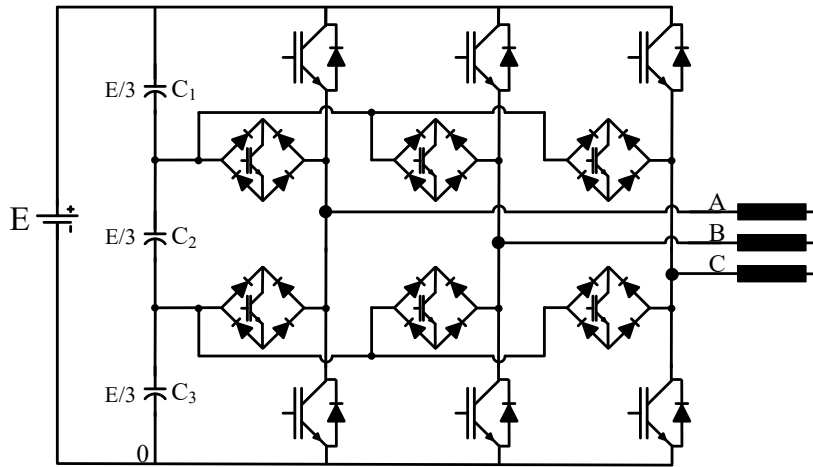


Fig. 38 Three-phase four-level inverter proposed in [116].

As highlighted above, the multilevel inverters are salient candidates for several applications in both renewable energy systems and motor drives. Further, MLIs become a featured solution for improving the power quality in power systems. They can operate as static synchronous compensators (STATCOMs) and unified power quality conditioners (UPQCs), handling reactive power demand, harmonics compensation, and voltage disturbances (e.g. sag/swell). Flying-capacitor MLI (FCMLI), diode-clamped MLI (DCMLI), and cascaded H-bridge MLI (CHBMLI) are widely used to form multilevel-based STATCOMs [117-121]. Both FCMLIs and DCMLIs have DC-link shared among the three phases, improving the compensation of the negative-sequence currents as compared to the star-connected CHBMLI. These two topologies have a problem of poor modularity and using high capacitor and diode counts. The CHBMLIs have a remarkable feature of modularity, making them more attractive than FCMLIs and DCMLIs. However, connecting the CHB in a star-configuration reduces the compensation capability of the negative-sequence current. This drawback is solved by applying a delta-configuration of CHB, but this would boost the arming voltage of the converter, increasing the submodule count or rating the components [122].

Scalability and transformerless capability of the modular multilevel converter (MMC) make it reasonably competitive for replacing the conventional MLIs in high-voltage STATCOM applications [123]. Fig. 39 shows the conventional MMC-based STATCOM configuration, consisting of three-phase legs connected to two bulk capacitors (C_U and C_L). Each phase has two arms (lower and upper arms) and two inductors (L_{a1} and L_{a2}). For constructing both arms, several submodules are cascaded, typically a flying capacitor connected to either half-bridge (HB) or full-bridge (FB). The arm inductors L_{a1} - L_{a6} are necessary for limiting the current during faults and reducing the harmonic content in the circulating current. Balancing the voltage of flying capacitors is a significant challenge in STATCOM-based MMC, requiring complex control algorithms and a high number of voltage sensors [122-124]. The authors in [122] proposed a solution to keep the capacitor voltage in different submodules balanced, reducing

the sensor count and computational burden in control algorithms. The conventional arm structure based on cascaded HB cells is depicted in Fig. 40 (a), while Fig. 40 (b) shows the proposed one. In the proposed structure, a balancing branch (BB), formed by a series connection of low-power rating inductor and diode, is added between the neighbored cells. The diodes are used to clamp the voltage of capacitors naturally from the bottom cell upwards. Using inductors is mandatory to suppress the current pulses during abnormal conditions, protecting the switches and reducing the diode current ratings. According to the proposed solution, only the voltage of the capacitor in either the top or bottom of each arm must be controlled and monitored. The remarkable features of simplifying voltage balancing control and low sensor count come with the cost of increasing the component count (diodes and inductors) as compared to the conventional MMC.

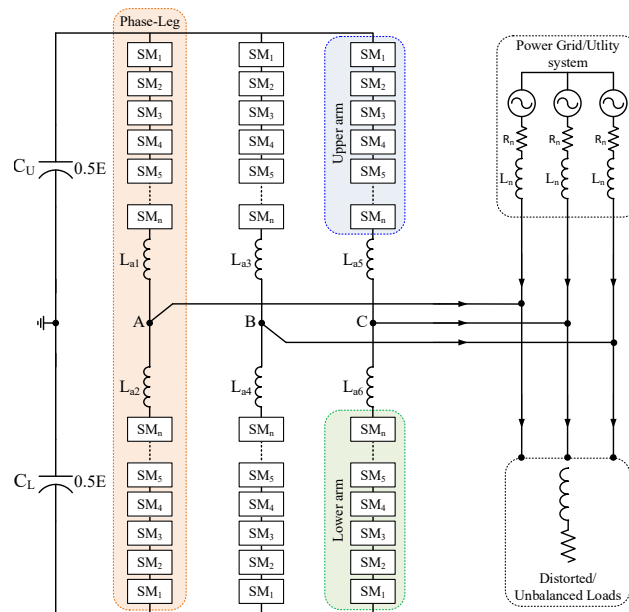


Fig. 39 MMC-based STATCOM configuration.

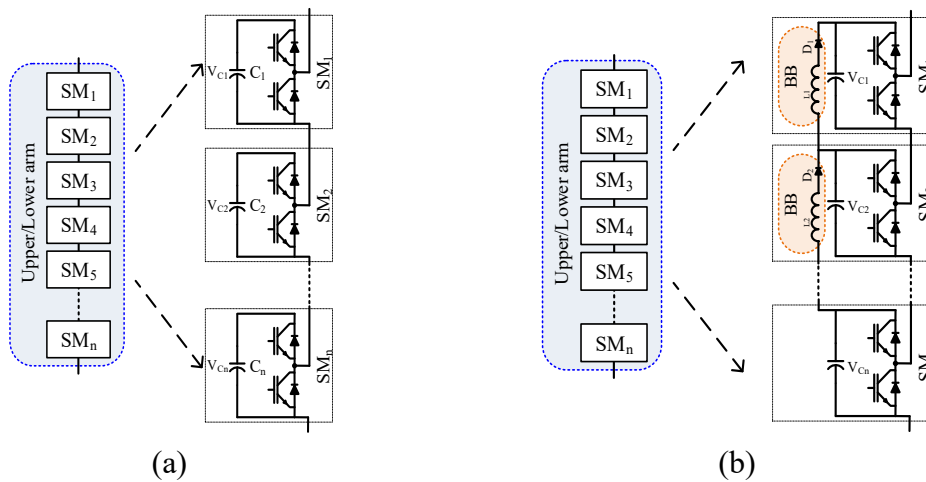


Fig. 40 Arm structures based on half-bridge cells for MMC-based STATCOM. When capacitors voltage is balanced, $V_{C_i} = E/n$ where $i = 1, 2, \dots, n$. (a) Conventional structure of an arm in MMC-based STATCOM. (b) Proposed diode-clamped arm structure in [122] for MMC-based STATCOM.

To synthesise a desired multilevel AC voltage, a large count of floating capacitors is required in the MMC-based STATCOM, in which electrolytic capacitors are normally used to fulfil the high-capacitance requirements for buffering energy variations. Besides the well-known disadvantages of using a large number of capacitors [125], the electrolytic ones have a higher failure rate than other components in the systems [125-127]. To lower capacitor count and voltage rating of switches while producing higher voltage levels, some transformer-based solutions were proposed in [128, 129]. The authors in [128] introduced a four-level STATCOM configuration based on cascading two conventional two-level inverters as depicted in Fig. 41. Two corresponding legs of the two-level inverters are connected through one winding of a three-phase transformer. The low-voltage (LV) windings are used for cascading the two inverters while the three windings of the high-voltage (HV) side are connected to the grid terminals. To obtain a four-level operation, the voltages of the two DC-link capacitors are regulated to have asymmetrical values. One three-phase transformer is needed in addition to twelve switches and two capacitors. This topology has a simple structure and a low component count. However, the demerit of using a three-phase transformer (in term of size and cost) restricts its applicability, being more advantageous in low-capacity STATCOMs. A modified topology of the presented STATCOM configuration in [128], was proposed in [129]. Three two-level inverters and a three-phase transformer are used to construct the proposed STATCOM in Fig. 42. One leg in each inverter is used to connect the three inverters in a Y-configuration, while the remaining two legs are connected to different windings in the low-voltage side of the transformer. This connection makes the applied AC voltage of the transformer windings double the DC voltage across the capacitor. Under the regulation of the capacitor voltages at symmetrical values, the proposed configuration produces five voltage levels of $-2E$, $-E$, 0 , E , and $2E$ across each transformer winding, requiring one three-phase transformer, three capacitors, and eighteen switches. As compared to [128], the proposed topology needs one extra two-level inverter (i.e. one capacitor and six switches). Consequently, the applied voltage across the transformer winding is increased from 1.33 to double the capacitor voltage while producing five levels instead of four, lowering both THD value and component ratings. It is worth mentioning that the topologies in [128, 129] have been introduced for driving open-end winding induction motors [130, 131].

Another significant application of the MLIs in the field of power quality is constructing more competitive unified power quality conditioners (UPQCs). Briefly, UPQC consists of two compensators, in which the series compensator is responsible for handling voltage related issues (e.g. voltage sag/swell, flickers, etc.) and the shunt compensator is to tackle issues of harmonic and reactive power compensations [132-140]. Several configurations for UPQCs based on conventional MLI topologies were proposed in [133-136], suffering from a high component count or limited level count due to using many capacitors or diodes or transformers. The modular multilevel converter (MMC) concept was applied to obtain UPQCs with higher power levels [137-139]. Fig. 43 shows the UPQC based on two MMCs. The MMC-A acts as a series compensator, being connected to the

grid through a series injection transformer (T_C), while three coupling inductors (L_a , L_b , and L_c) are used to interface the shunt compensator (i.e. MMC-B) to the grid. It is worth noting that the coupling inductors can be used for smoothing the currents. Attractive features, namely high-quality waveforms, fast current control, and easy scalability of voltage and current, are important in applying MMC to UPQC. On the other hand, using many floating capacitors as storage elements, increasing size and failure rates, is its main limitation for UPQCs.

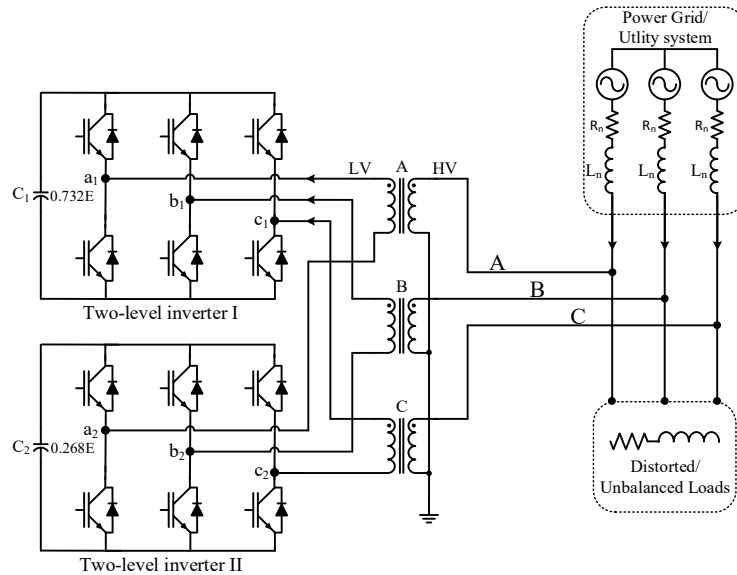


Fig. 41 STATCOM based on cascading two two-level VSIs in [128].

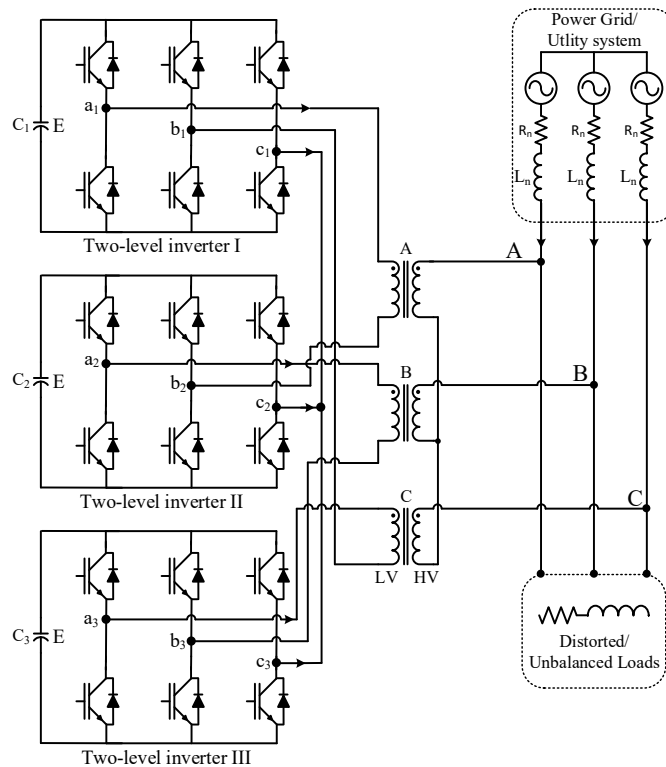


Fig. 42 STATCOM based on three two-level VSIs in [129].

Another MLI-based UPQC was proposed in [140], and the proposed configuration is shown in Fig. 44. It consists of two identical MLIs, being connected in back-to-back assembly. Each inverter requires twenty-four switches and three floating capacitors for producing five levels. Two capacitors C_1 and C_2 are used for constructing a DC-link with a middle point called M . As compared to the introduced diode-clamped UPQC in [136], the proposed UPQC configuration saves 36 diodes, but needs eight capacitors instead of four. Although both UPQC configurations require the same switch count, the total standing voltage of switches in [140] is higher than that in [136]. Further, both must use a sophisticated control for balancing capacitors voltage at specific values.

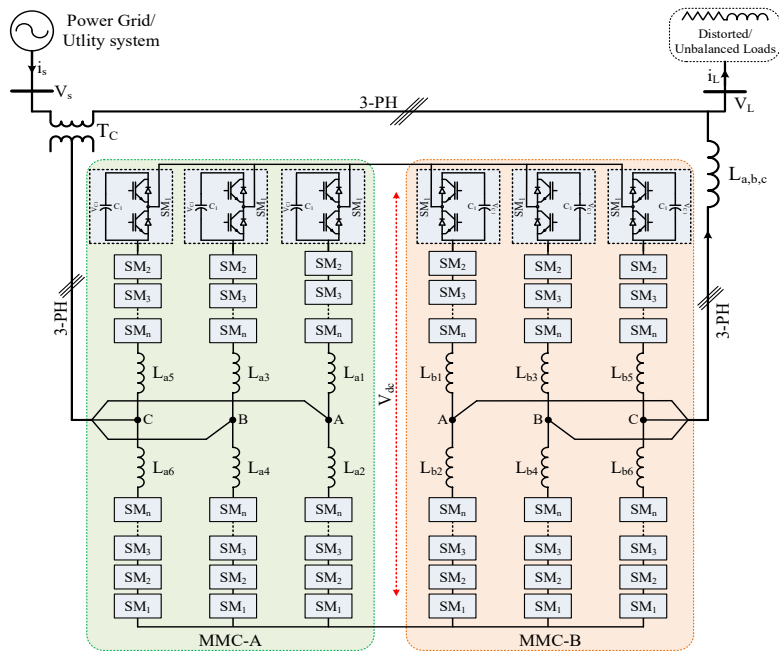


Fig. 43 Configuration of MMC-based UPQC in [137-139].

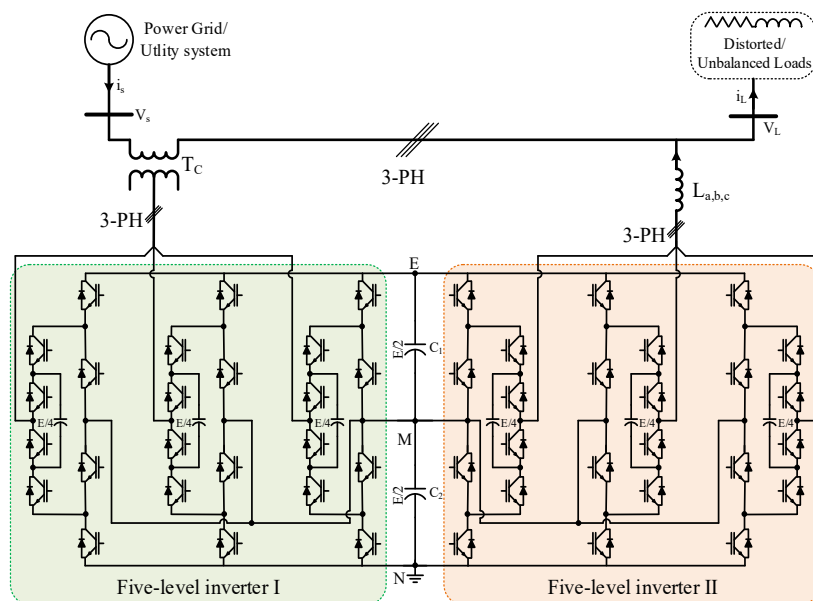


Fig. 44 Configuration of UPQC implemented by the back-to-back connection of two five-level inverters [140].

III. THE PROPOSED BENCHMARK FOR COMPARING MULTILEVEL INVERTER TOPOLOGIES

A. EXISTING FACTORS FOR COMPARING MULTILEVEL TOPOLOGIES

Over the past few years, several MLI topologies have been proposed for improving the power conversion efficiency, system reliability, power quality in several applications. The significant number and diversity of the proposed topologies allow the customers to select the suitable one to their needs, but selecting the best one is always a challenge. Different aspects and aims are set in a design process, for example, low semiconductors count, low passive elements, isolation features, boosting abilities, modularity, etc. To make the comparative process easier and more efficient for both industry and academia, two strategies have been presented in [34, 35]. The strategy in [34] is based on the level-number per switch ratio (LSR) for comparing different MLIs. As described in (1), the *LSR* is calculated by the number of levels N over the switch count (N_{sw}), indicating number of levels generated by each switch. Accordingly, topologies with higher *LSR* are better than those with a lower one from the switch count point of view.

$$LSR = \frac{N}{N_{sw}} \quad (1)$$

LSR cannot figure out other component counts, e.g. capacitors (N_C), inductors (N_L), diodes (N_D), transformers (N_{Trf}), DC sources (N_{DC}), and other components (N_X). To overcome this drawback, the component per level factor (*CLF*) was proposed in [35] as a comparative factor. Instead of counting only switches, *CLF* is to count all the used components for producing one level, as calculated in (2). Therefore, it can be used to compare MLI topologies by the total component count. A reduced component circuit has a lower *CLF*.

$$CLF = \frac{N_C + N_D + N_L + N_{sw} + N_{DC} + N_{TRF} + N_X}{N} \quad (2)$$

The proposed MLI topologies in [36-56, 58-83, 85, 86, 92, 95-97, 101-104, 107, 109-116, 141-156] are compared together by using the two comparative factors *LSR* and *CLF* in terms of component count. The compared MLIs in this work are named from $T1$ to $T120$, in which the same reference can be seen in different categories because some authors have proposed two or more configurations in one publication. Tables I and II show comparisons for single-phase MLI topologies of single/symmetrical and asymmetrical DC sources in literature while the three-phase MLIs are compared and summarized in Tables III and IV. The presented topologies were very diverse, in which some of them can generate N levels while the others were designed for a specific voltage level number. Therefore, to make a fair comparison, they are grouped based on the number of levels, for example, group A represents five-level topologies that use either symmetrical or single DC sources. The last row of each group highlights a topology that has the least component count. In the comparison, several aspects are adopted/assumed: each battery or PV string is counted as one DC source, and each winding of a coupled

TABLE I
COMPONENT REQUIREMENT FOR SINGLE-PHASE MULTILEVEL INVERTERS IN [36-47, 49, 51-56, 59, 61-63, 65-67, 70-73, 75, 77, 80, 81, 83, 85, 86, 102, 141, 142]

	Topology	In	N	N_{DC}	N_{SW}	N_D	N_L	N_{Cap}	N_{Trf}	N_{Total}	LSR	CLF
Group A	T120	[85]	5	1	8	6	4	4	0	23	0.63	4.60
	T38	[37]	5	2	8	4	2	3	0	19	0.63	3.80
	T119	[86]	5	1	8	3	2	4	0	18	0.63	3.60
	T48	[70]	5	1	12	0	0	4	0	17	0.42	3.40
	T59	[77]	5	1	10	0	0	4	0	15	0.50	3.00
	T34	[39]	5	2	4	4	2	2	0	14	1.25	2.80
	T37	[38]	5	2	4	4	2	2	0	14	1.25	2.80
	T54	[36]	5	1	6	3	1	2	0	13	0.83	2.60
	T47	[75]	5	1	6	2	0	3	0	12	0.83	2.40
	T52	[71]	5	2	8	0	0	2	0	12	0.63	2.40
	T43 ^a	[65]	5	2	7	2	0	0	0	11	0.71	2.20
	T51	[72]	5	1	6	0	0	3	0	10	0.83	2.00
Group B	T49	[73]	7	1	16	0	0	3	0	20	0.43	2.85
	T58	[59]	7	1	8	4	0	3	0	16	0.88	2.29
	T30	[66]	7	1	7	2	0	3	0	13	1.00	1.86
	T45	[67]	7	3	10	0	0	0	0	13	0.70	1.86
	T65	[141]	7	1	8	0	0	4	0	13	0.88	1.86
	T110	[83]	7	1	9	0	0	3	0	13	0.78	1.86
	T24 ^a	[62]	7	3	6	2	0	0	0	11	1.17	1.57
	T26 ^a	[61]	7	3	8	0	0	0	0	11	0.88	1.57
T46	[63]	7	3	7	1	0	0	0	11	1.00	1.57	
Group C	T35	[39]	9	1	8	8	4	2	0	23	1.13	2.56
	T1	[43]	9	1	16	0	0	0	4	21	0.56	2.33
	T56	[56]	9	1	10	4	1	4	0	20	0.90	2.22
	T44 ^a	[65]	9	4	9	4	0	0	0	17	1.00	1.89
	T110	[83]	9	1	12	0	0	4	0	17	0.75	1.89
	T33	[42]	9	1	12	0	0	3	0	16	0.75	1.78
	T36	[39]	9	1	6	4	2	2	0	15	1.50	1.67
	T17	[54]	9	1	8	0	0	2	4	15	1.13	1.67
	T40	[40]	9	2	10	0	2	0	0	14	0.90	1.56
	T41	[40]	9	2	10	0	2	0	0	14	0.90	1.56
	T42	[40]	9	2	10	0	2	0	0	14	0.90	1.56
	T53	[41]	9	1	10	0	0	3	0	14	0.90	1.56
	T55	[55]	9	1	9	2	0	2	0	14	1.00	1.56
	T2	[44]	9	1	10	0	0	3	0	14	0.90	1.56
	T3	[45]	9	1	10	0	0	3	0	14	0.90	1.56
T111	[80]	9	4	10	0	0	0	0	14	0.90	1.56	
T25 ^a	[62]	9	4	7	2	0	0	0	13	1.29	1.44	

^a Addressed for symmetrical mode alone, more details for their operation under asymmetrical mode (DC sources have asymmetrical values) can be found in [61, 62, 65]. Only number of levels will be changed while using same component count.

TABLE I
COMPONENT REQUIREMENT FOR SINGLE-PHASE MULTILEVEL INVERTERS IN [36-47, 49, 51-56, 59, 61-63, 65-67, 70-73, 75, 77, 80, 81, 83, 85, 86, 102, 141, 142] (Continued)

Group C (Continued)	T39	[40]	9	2	8	0	2	0	0	12	1.13	1.33
	T62	[102]	9	2	8	0	0	2	0	12	1.13	1.33
	T14	[52]	9	2	8	0	0	0	1	11	1.13	1.22
	T64	[142]	9	2	8	0	0	1	0	11	1.13	1.22
	T8	[49]	9	1	8	0	0	0	1	10	1.13	1.11
	T16	[53]	9	1	8	0	0	0	1	10	1.13	1.11
Group D	T117	[81]	15	1	26	0	0	7	0	34	0.58	2.27
	T46	[63]	15	7	13	3	0	0	0	23	1.15	1.53
	T5	[46]	15	1	8	0	0	2	3	14	1.88	0.93
	T13	[51]	15	1	8	0	0	0	2	11	1.88	0.73
Group E	T6	[47]	27	1	12	0	0	0	3	16	2.25	0.59
	T14	[52]	27	2	12	0	0	0	2	16	2.25	0.59
	T15	[52]	27	2	12	0	0	0	2	16	2.25	0.59

TABLE II
COMPONENT REQUIREMENT FOR ASYMMETRICAL SINGLE-PHASE MULTILEVEL INVERTERS IN [48, 50, 51, 58, 60, 64, 66, 68, 69, 74, 76, 78-80, 82, 102, 143]

	Topology	In	N	N_{DC}	N_{Sw}	N_D	N_L	N_{Cap}	N_{Trf}	N_{Total}	LSR	CLF
Group F	T115	[74]	5	2	6	1	0	0	0	9	0.83	1.8
Group G	T61-a	[102]	7	2	8	0	0	2	0	12	0.88	1.71
	T4	[143]	7	2	8	0	0	0	0	10	0.88	1.43
Group H	T112	[68]	9	2	10	0	0	0	0	12	0.90	1.33
	T116	[82]	9	2	8	0	0	0	0	10	1.12	1.11
Group I	T63	[102]	13	4	16	0	0	4	0	24	0.81	1.85
	T61-a	[102]	13	2	14	0	0	5	0	21	0.93	1.62
	T19	[76]	13	4	10	0	0	0	0	14	1.30	1.08
Group J	T113	[69]	15	3	9	4	0	0	0	16	1.67	1.06
	T61-b	[102]	15	2	10	0	0	3	0	15	1.50	1.00
	T60	[143]	15	3	10	0	0	0	0	13	1.50	0.87
	T18	[79]	15	3	8	0	0	0	0	11	1.88	0.73
	T12	[51]	15	2	8	0	0	0	1	11	1.88	0.73
Group K	T22 ^a	[60]	17	2	10	2	0	2	0	16	1.70	0.94
	T111	[80]	17	4	10	0	0	0	0	14	1.70	0.82
	T29	[64]	17	4	10	0	0	0	0	14	1.70	0.82
Group L	T61-b	[102]	19	2	12	0	0	4	0	18	1.58	0.95
	T7	[48]	19	2	10	2	0	0	2	16	1.90	0.84
	T9	[50]	19	2	12	0	0	0	2	16	1.58	0.84

^aAddressed for asymmetrical mode alone, more details for their operation under symmetrical mode (DC sources have symmetrical values) can be found in [51, 60, 78]. Only number of levels will be changed while using same component count.

TABLE II
 COMPONENT REQUIREMENT FOR ASYMMETRICAL SINGLE-PHASE MULTILEVEL
 INVERTERS IN [48, 50, 51, 58, 60, 64, 66, 68, 69, 74, 76, 78-80, 82, 102, 143]
 (Continued)

Group M	T61-a	[102]	23	2	24	0	0	10	0	36	0.96	1.57
	T31	[66]	23	2	13	3	0	5	0	23	1.77	1.00
	T61-b	[102]	23	2	14	0	0	5	0	21	1.64	0.91
Group N	T63	[102]	25	8	32	0	0	8	0	48	0.78	1.92
	T61-a	[102]	25	2	26	0	0	11	0	39	0.96	1.56
	T32 ^a	[78]	25	4	10	8	0	0	0	22	2.50	0.88
Group O	T6-b	[102]	31	2	18	0	0	7	0	27	1.72	0.87
	T28	[64]	31	6	14	0	0	0	0	20	2.21	0.65
Group P	T63	[102]	49	16	64	0	0	16	0	96	0.77	1.96
	T23 ^a	[60]	49	3	14	3	0	3	0	23	3.50	0.47
	T11 ^a	[51]	49	2	12	0	0	0	2	16	4.08	0.33
	T116	[82]	49	4	12	0	0	0	0	16	4.08	0.33
Group Q	T63	[102]	55	18	72	0	0	18	0	108	0.76	1.96
	T21	[58]	55	3	44	0	0	7	0	54	1.25	0.98
	T61-b	[102]	55	2	30	0	0	13	0	45	1.83	0.82

^aAddressed for asymmetrical mode alone, more details for their operation under symmetrical mode (DC sources have symmetrical values) can be found in [51, 60, 78]. Only number of levels will be changed while using same component count.

TABLE III
 COMPONENTS REQUIREMENT FOR ASYMMETRICAL THREE-PHASE MULTILEVEL INVERTER
 TOPOLOGIES IN [102, 109-112, 114, 143, 149, 156]

	Topology	In	N	N_{DC}	N_{SW}	N_D	N_L	N_{Cap}	N_{Trf}	N_{Total}	LSR	CLF
Group R	T81	[112]	4	3	16	12	0	0	0	31	0.25	7.75
	T82	[114]	4	2	24	0	0	0	0	26	0.17	6.50
Group S	T80	[111]	7	6	18	24	0	0	0	48	0.39	6.86
	T86	[102]	7	6	24	0	0	6	0	36	0.29	5.14
	T74	[143]	7	6	24	0	0	0	0	30	0.29	4.29
Group T	T81	[112]	10	9	28	12	0	0	0	49	0.36	4.90
	T79	[110]	10	8	24	0	0	0	0	32	0.42	3.20
Group U	T80	[111]	11	8	24	48	0	0	0	80	0.46	7.27
	T88	[102]	11	6	24	0	0	6	0	36	0.46	3.27
Group V	T80	[111]	15	10	30	72	0	0	0	112	0.50	7.47
	T75	[143]	15	9	30	0	0	0	0	39	0.50	2.60
Group W	T81	[112]	17	16	42	12	0	0	0	70	0.40	4.12
	T89	[156]	17	6	36	0	0	9	0	51	0.47	3.00
Group X	T80	[111]	19	12	36	96	0	0	0	144	0.53	7.58
	T85	[109]	19	13	36	0	0	14	0	63	0.53	3.32
Group Y	T81	[112]	31	30	70	12	0	0	0	112	0.44	3.61
	T76	[143]	31	12	36	0	0	0	0	48	0.86	1.55
Group Z	T71	[149]	33	4	36	0	0	6	3	49	0.92	1.48
	T90	[149]	33	6	36	0	0	6	0	48	0.92	1.45

TABLE IV
 COMPONENT REQUIREMENT FOR THREE-PHASE MULTILEVEL INVERTERS IN [39, 44, 45, 92, 95-97, 101-104, 107, 109, 110, 113, 115, 116, 141, 142, 144-148, 150-155]

	Topology	In	N	N_{DC}	N_{Sw}	N_D	N_L	N_{Cap}	N_{Trf}	N_{Total}	LSR	CLF
Group A1	T94	[95]	3	2	14	10	2	2	0	30	0.21	10.00
	T103	[96]	3	1	12	2	4	4	0	23	0.25	7.67
	T107	[150]	3	1	14	4	1	2	0	22	0.21	7.33
	T93	[107]	3	1	16	0	0	4	0	21	0.19	7.00
	T104	[97]	3	1	12	3	1	4	0	21	0.25	7.00
	T114	[116]	4 ^a	1	12	24	0	3	0	40	0.58	5.71
	T118	[92]	3	1	12	0	0	2	0	15	0.25	5.00
	T96	[115]	3	2	12	0	0	0	0	14	0.25	4.67
Group B1	T97	[103]	5	2	24	6	0	9	0	41	0.21	8.20
	T108	[151]	5	1	21	12	0	5	0	39	0.24	7.80
	T77	[39]	5	2	12	12	6	2	0	34	0.42	6.80
	T99	[154]	5	2	20	6	0	2	0	30	0.25	6.00
	T69	[147]	5	2	24	0	0	0	3	26	0.21	5.80
	T100	[154]	5	2	20	0	0	2	0	24	0.25	4.80
	T105	[152]	5	1	18	0	0	4	0	23	0.28	4.60
	T67	[144]	5	1	16	0	0	2	2	19	0.31	4.20
	T109	[153]	5	1	15	0	0	3	0	19	0.33	3.80
Group C1	T66	[145]	5	1	12	0	0	2	2	15	0.42	3.40
	T78	[110]	6	8	24	0	0	0	0	32	0.25	5.33
Group D1	T102	[104]	6	1	24	0	0	6	0	31	0.25	5.17
	T98	[155]	7	2	36	0	0	9	0	47	0.19	6.71
Group E1	T106	[141]	7	1	24	0	0	8	0	33	0.29	4.71
	T91	[113]	9	2	42	0	0	9	0	53	0.21	5.89
	T95	[101]	9	3	36	0	0	12	0	51	0.25	5.67
	T72	[44]	9	1	30	0	0	9	3	40	0.30	4.78
	T73	[45]	9	1	30	0	0	9	3	40	0.30	4.78
	T83	[109]	9	7	24	0	0	8	0	39	0.38	4.33
	T101	[142]	9	6	24	0	0	9	0	39	0.38	4.33
	T87	[102]	9	6	24	0	0	6	0	36	0.38	4.00
T70	[148]	9	2	16	0	0	0	6	18	0.56	2.67	
Group F1	T78	[110]	15	26	60	0	0	0	0	86	0.25	5.73
	T84	[109]	15	13	36	0	0	14	0	63	0.42	4.20
Group G1	T84	[109]	21	19	48	0	0	20	0	87	0.44	4.14
	T68	[146]	21	1	48	0	0	0	12	49	0.44	2.90
Group H1	T69	[147]	49	24	156	0	0	0	3	180	0.31	3.73
	T92	[113]	49	3	84	6	0	18	0	111	0.58	2.27

^a It can generate four levels, so it is inserted in the closest group, i.e. 3-level inverters group.

inductor is considered one inductor, input and output filter components are discounted, a three-phase transformer is calculated as three single-phase transformers and the same for multi-winding/secondary transformers cases. The unidirectional switch is considered as the base for counting the switch number, so bidirectional ones are disassembled into their primary components.

Based on Tables I-IV, the drawbacks of using *LSR* for comparing MLIs have been solved by *CLF*. However, important factors like component ratings have been ignored when computing *CLF* values for the compared circuits since the *CLF* alone is not able to compare the used components in term of ratings. One device with a voltage rating of $10E$ has been equally counted as a device with the voltage rating of $0.5E$. Consequently, a new indicator or method for comparing MLI topologies more accurately is very important for both industry and academia to select the best circuit in term of the component count.

B. THE PROPOSED COMPARATIVE FACTOR: COMPONENT FOR EACH LEVEL (CEL)

In this section, a new method is proposed to compare MLI topologies. First, the MLI components are subdivided into two groups: semiconductors and passive elements. The semiconductor group includes switches and diodes while capacitors, inductors, and transformers are classified as passive elements. Second, for simplicity, the peak current passing through each component is assumed to be the same and equal to the load current. Further, the peak voltage (*VPK*) is considered as an indicator for the rating of the component.

For calculating the equivalent semiconductor count NE_{SEMI} , the total standing voltage (TSV_{SEMI}) for NE_{SEMI} elements is calculated as in (3). Afterwards, NE_{SEMI} is defined by TSV_{SEMI} and the base value of the voltage (V_{BASE}) in (4). For the passive elements, several parameters, such as capacitance, inductance, equivalent resistance, are used in the evaluation. Each topology has different specifications based on input/output waveforms or depending on facility conditions of research groups. In the proposed comparative strategy, the voltage is a dominant factor as the current has been assumed equal to the load current. The equivalent numbers of capacitors NE_C , inductors NE_L , transformers NE_{Trf} , and DC sources NE_{DC} are calculated by (5)-(8), respectively. For example, if topology T_X requires two DC sources of E and $2E$ volt, the number of DC sources N_{DC} is 2, while the equivalent number NE_{DC} is equal to three ($NE_{DC}=(E+2E)/E$). The same rule can be applied for the rest of the used components. The total equivalent component count NE_{Total} and *CEL* are defined by (9) and (10), respectively.

$$TSV_{SEMI} = \sum_{i=1}^{N_{SEMI}} VPK_i \quad (3)$$

$$NE_{SEMI} = \frac{TSV_{SEMI}}{V_{BASE}} \quad (4)$$

$$NE_C = \frac{\sum_{i=1}^{N_C} VPK_i}{V_{BASE}} \quad (5)$$

$$NE_L = \frac{\sum_{i=1}^{N_L} VPK_i}{V_{BASE}} \quad (6)$$

$$NE_{TRF} = \frac{\sum_{i=1}^{N_{TRF}} VPK_i}{V_{BASE}} \quad (7)$$

$$NE_{DC} = \frac{\sum_{i=1}^{N_{DC}} VPK_i}{V_{BASE}} \quad (8)$$

$$NE_{TOTAL} = NE_{SEMI} + NE_C + NE_L + NE_{TRF} + NE_{DC} \quad (9)$$

$$CEL = \frac{NE_{TOTAL}}{N} \quad (10)$$

The passive elements in the MLI topologies, such as capacitors and inductors, have distinctive natures as compared to other components since they store energy either in magnetic or electric fields. An additional comparative factor, namely stored energy factor (SEF), is proposed to take their stored energy (SE) into consideration when comparing topologies beside their equivalent numbers. The total stored energy (TE) of stored energy elements (N_{SE}) is calculated in (11) and used to obtain the proposed *SEF* in (12).

$$TE = \sum_{i=1}^{N_{SE}} SE_i \quad (11)$$

$$SEF = \frac{TE}{TE_{BASE}} \quad (12)$$

where SE_i is the stored energy on a passive element i in a topology. TE_{BASE} is the total stored energy base value. The value of the TE_{BASE} can be the total stored energy of an interested or proposed topology.

The *SEF* can be calculated for different stored energy elements in a compared topology T_x , indicating the stored energy in a percentage. *SEF* should be accompanied to the equivalent counts of the stored energy elements (i.e. NE_C and NE_L) when comparing T_x with other topologies. These factors allow for a fairer comparison of topologies that contain stored energy elements. For example, two

MLI topologies (T_A and T_B) use capacitors. T_A has two capacitors of 1 mF and voltage rating of 100 V, while T_B has three capacitors, (two of 0.25 mF and one of 0.5 mF) and all of the capacitors have voltage rating of 75 V. The equivalent count of the capacitor is defined by (5), and their $SEFs$ are calculated by (11) and (12). The equivalent capacitor counts of T_A and T_B are 2 and 2.25, respectively (V_{BASE} is selected at 100 V). The $SEFs$ of T_A and T_B are 1 and 0.28, respectively (TE for T_A is " $2*0.5 * 1e^{-3}*100^2$ " and for T_B is " $(2*0.5*0.25e^{-3}*75^2) + (0.5*0.5e^{-3}*75^2)$ ", TE_{BASE} is selected to be T_A stored energy). Accordingly, T_A has a less equivalent count of capacitors (2 instead of 2.25) as compared to T_B , but T_B has a lower SEF (0.28 instead of 1). Although the topology T_B requires a higher equivalent capacitor count, the capacitors store 28.1% of the stored energy in T_A , affecting the cost and size of the capacitors. It is worth mentioning that the same procedure can be applied to inductors as well.

To verify the effectiveness of the proposed factor CEL over the existing factor in ranking MLIs in term of component counts, five-level topologies $T99$, $T100$, CHB, NPC, and FC are selected in a comparative study as shown in Table V. CHB, NPC, and FC are the conventional MLIs, while $T99$ and $T100$ are novel MLI topologies in [154]. A fair comparison among the selected topologies can be achieved because both number and value of the output voltage levels are the same for all of them (i.e. five levels of $-0.25E$, $-0.5E$, 0 , $0.25E$, and $0.5E$ volt). Table V also shows the voltage rating/stress for all components in the case-study topologies.

Topology $T99$ shown in Fig. 45 is selected as an example to clarify the CEL calculation. It consists of two DC sources, twenty switches, two capacitors, and six diodes. It requires eight switches with a voltage rating of $0.25E$ and twelve switches with $0.5E$, in addition to six diodes with a rating of $0.5E$ and two $0.25E$ capacitors. It does not have any transformers or inductors. For calculating the equivalent semiconductor count, NE_{SEMI} , first (3) is used for obtaining TSV_{SEMI} value, and then (4) is used to define NE_{SEMI} . TSV_{SEMI} is $11E$ ($= 8*0.25E+12*0.5E+6*0.5E$), so the value of NE_{SEMI} is 11. Using (5) and (8), NE_C and NE_{DC} can be calculated as $((0.25E+0.25E)/E)$ and $((0.5E+0.5E)/E)$, respectively. Using (9) and the obtained values of NE_{SEMI} , NE_{DC} and NE_C , results in the total component count of 12.5. Finally, CEL is calculated by using (10) to be 2.5. For the $T100$, CHB, and FC, the same procedure can be repeated.

In Table V, the differences between the existing method and the proposed one can be well observed. For example, in $T99$, the CLF factor results in the total component count N_{Total} of 30 regardless of their voltage rating while NE_{Total} is only 12.5 when using CEL factor. Without considering the component voltage rating or based on CLF values alone, the CHB requires more components than those in $T100$ since its CLF is higher than that of $T100$. However, when considering the voltage rating by the proposed indicator CEL , the total equivalent component count of the CHB is lower than that of $T100$ since the CEL of CHB is smaller than that of $T100$.

As mentioned before, in addition to the equivalent numbers of the used components in each topology to find CEL values, the stored energy factor (SEF) is recommended for a better description of stored energy elements in the compared topologies. Table VI lists the total energy TE and SEF for each topology based on

(11) and (12). It is worth noting that the listed $SEFs$ are a function of the utilised capacitors in the circuits, and not given as numerical values. Obtaining the numerical values requires detailed parameters of rated power, operating voltage, switching frequency, and voltage ripple, etc. It is important to consider all parameters that affect the stored energy element selection during the design process, when using SEF for obtaining a fairer comparison.

TABLE V
USING CLF AND CEL FOR COMPARING THE FIVE-LEVEL INVERTERS IN [154] AND THE THREE BASIC MLI TOPOLOGIES

Topology	DC sources			Switching devices			Diodes			Capacitors			Existing method		Proposed method	
	E/4	E/2	E	E/4	E/2	E	E/4	E/2	3E/4	E/4	E/2	3E/4	N_{Total}	CLF	NE_{Total}	CEL
T99	0	2	0	8	12	0	0	6	0	2	0	0	30	6	12.5	2.5
T100	0	2	0	8	6	6	0	0	0	2	0	0	24	4.8	12.5	2.5
CHB	6	0	0	24	0	0	0	0	0	0	0	0	30	6	7.5	1.5
NPC	0	0	1	24	0	0	6	6	6	4	0	0	47	9.4	17	3.4
FC	0	0	1	24	0	0	0	0	0	7	3	3	38	7.6	12.5	2.5

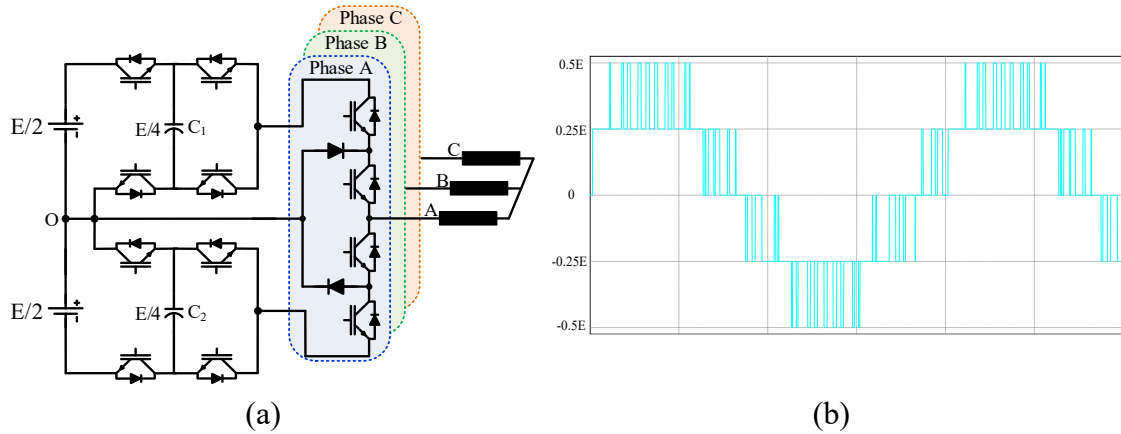


Fig. 45 Five-level three-phase topology T99 [154]. (a) Circuit configuration. (b) Output pole voltage for the compared MLI circuits in Table V.

The comparison suggests that each topology should be evaluated by some of these factors, i.e. NE_{SEMI} , NE_{DC} , NE_C , NE_L , NE_{Trf} , SEF , and CEL , to highlight its merits, allowing for finding the most suitable application. For example, in PV farms, NE_{DC} is less important than that in motor drives while NE_C , NE_L , NE_{Trf} , and SEF should be reduced for more compact designs. For control simplicity, NE_{SEMI} and NE_C have the salient effects as compared to other factors. Finally, the CEL factor is the most important for having a reduced component count regardless of distinct features in each topology.

TABLE VI
CALCULATION OF THE STORED ENERGY FACTOR FOR THE FIVE-LEVEL INVERTERS IN [154] AND THE THREE BASIC MLI TOPOLOGIES

Topology	Capacitors ^a			Stored energy factor calculation		
	E/4	E/2	3E/4	TE _{BASE}	TE	SEF
T99	2	0	0	$E^2/32 (C_{A1}+C_{A2})$	$E^2/32 (C_{A1}+C_{A2})$	1
T100	2	0	0	$E^2/32 (C_{A1}+C_{A2})$	$E^2/32 (C_{B1}+C_{B2})$	$(C_{B1}+C_{B2})/(C_{A1}+C_{A2})$
CHB	0	0	0	$E^2/32 (C_{A1}+C_{A2})$	0	0
NPC	4	0	0	$E^2/32 (C_{A1}+C_{A2})$	$E^2/32 \sum_{i=1}^4 C_{Ci}$	$\sum_{i=1}^4 C_{Ci} / (C_{A1}+C_{A2})$
FC	7	3	3	$E^2/32 (C_{A1}+C_{A2})$	$0.4375E^2 \sum_{i=1}^{13} C_{Di}$	$14 \sum_{i=1}^{13} C_{Di} / (C_{A1}+C_{A2})$

^a C_{A1} and C_{A2} are the capacitors in T_{99} . C_{B1} and C_{B2} are the capacitors in T_{100} . C_{C1} , C_{C2} , C_{C3} , and C_{C4} are the capacitors in NPC. C_{D1} , C_{D2} , ..., C_{D12} , and C_{D13} are the capacitors in FC.

IV. CONCLUSION

This paper presented a review study for the recently developed topologies in terms of construction, salient features and limitations, giving guidelines to further improve the current multilevel topologies more efficiently and compactly. A detailed comparison in terms of switch, diode, capacitor, inductor, transformer count was performed and systematically summarized in tables. New comparative factors - component for each level (CEL) and stored energy factor (SEF) were introduced to compare MLI topologies more effectively. A comparative study was presented to verify the usefulness of the proposed factors for comparing multilevel inverters, making it easier in evaluating newer topologies in the future.

REFERENCES

- [1] M. Vijeh, M. Rezanejad, E. Samadaei, and K. Bertilsson, "A general review of multilevel inverters based on main submodules: structural point of view," *IEEE Trans. Power Electron.*, pp. 1-1, 2019.
- [2] K. K. Gupta, A. Ranjan, P. Bhatnagar, L. K. Sahu, and S. Jain, "Multilevel inverter topologies with reduced device count: a review," *IEEE Trans. Power Electron.*, vol. 31, no. 1, pp. 135-151, 2016.
- [3] P. R. Bana, K. P. Panda, R. T. Naayagi, P. Siano, and G. Panda, "Recently developed reduced switch multilevel inverter for renewable energy integration and drives application: topologies, comprehensive analysis and comparative evaluation," *IEEE Access*, vol. 7, pp. 54888-54909, 2019.
- [4] J. Rodriguez, L. Jih-Sheng, and P. Fang Zheng, "Multilevel inverters: a survey of topologies, controls, and applications," *IEEE Trans. Ind. Electron.*, vol. 49, no. 4, pp. 724-738, 2002.
- [5] M. A. Perez, S. Bernet, J. Rodriguez, S. Kouro, and R. Lizana, "Circuit topologies, modeling, control schemes, and applications of modular multilevel converters," *IEEE Trans. Power Electron.*, vol. 30, no. 1, pp. 4-17, 2015.

- [6] M. N. Raju, J. Sreedevi, R. P. Mandi, and K. S. Meera, "Modular multilevel converters technology: a comprehensive study on its topologies, modelling, control and applications," *IET Power Electron.*, vol. 12, no. 2, pp. 149-169, 2019.
- [7] M. Priya, P. Ponnambalam, and K. Muralikumar, "Modular-multilevel converter topologies and applications – a review," *IET Power Electron.*, vol. 12, no. 2, pp. 170-183, 2019.
- [8] D. Ronanki and S. S. Williamson, "Modular multilevel converters for transportation electrification: challenges and opportunities," *IEEE Trans. Transp. Electrif.*, vol. 4, no. 2, pp. 399-407, 2018.
- [9] S. Debnath, J. Qin, B. Bahrani, M. Saeedifard, and P. Barbosa, "Operation, control, and applications of the modular multilevel converter: a review," *IEEE Trans. Power Electron.*, vol. 30, no. 1, pp. 37-53, 2015.
- [10] A. Nami, J. Liang, F. Dijkhuizen, and G. D. Demetriades, "Modular multilevel converters for HVDC applications: review on converter cells and functionalities," *IEEE Trans. Power Electron.*, vol. 30, no. 1, pp. 18-36, 2015.
- [11] K. K. Gupta and S. Jain, "Comprehensive review of a recently proposed multilevel inverter," *IET Power Electron.*, vol. 7, no. 3, pp. 467-479, 2014.
- [12] S. Kouro *et al.*, "Recent advances and industrial applications of multilevel converters," *IEEE Trans. Ind. Electron.*, vol. 57, no. 8, pp. 2553-2580, 2010.
- [13] J. Rodriguez, S. Bernet, B. Wu, J. O. Pontt, and S. Kouro, "Multilevel voltage-source-converter topologies for industrial medium-voltage drives," *IEEE Trans. Ind. Electron.*, vol. 54, no. 6, pp. 2930-2945, 2007.
- [14] R. H. Baker and L. H. Bannister, "Electric power converter," U.S. Patent 3867643, 1975.
- [15] R. H. Baker, "Switching circuit," U.S. Patent 4210826, 1980.
- [16] A. Nabae, I. Takahashi, and H. Akagi, "A new neutral-point-clamped PWM inverter," *IEEE Trans. Ind. Appl.*, vol. IA-17, no. 5, pp. 518-523, 1981.
- [17] T. A. Meynard and H. Foch, "Multi-level conversion: high voltage choppers and voltage-source inverters," in *Proc. 23rd Annu. IEEE Power Electron. Spec. Conf.*, 1992, pp. 397-403
- [18] J. P. Lavieville, P. Carrere, and T. Meynard, "Electronic circuit for converting electrical energy, and a power supply installation making use thereof," U.S. Patent 5 668 711, 1997.
- [19] F. J. Chivite-Zabalza, P. Izurza, G. Calvo, and M. A. Rodríguez, "Voltage balancing control in 3-level neutral-point clamped inverters using triangular carrier PWM modulation for FACTS applications," in *Proc. 14th Eur. Conf. on Power Electron. and Appl.*, 2011, pp. 1-10
- [20] D. Soto and T. C. Green, "A comparison of high-power converter topologies for the implementation of FACTS controllers," *IEEE Trans. Ind. Electron.*, vol. 49, no. 5, pp. 1072-1080, 2002.
- [21] J. Jung, S. Cui, J. Lee, and S. Sul, "A new topology of multilevel VSC converter for a hybrid HVDC transmission system," *IEEE Trans. Power Electron.*, vol. 32, no. 6, pp. 4199-4209, 2017.
- [22] M. B. Ghat and A. Shukla, "A new H-bridge hybrid modular converter (HBHMC) for HVDC application: operating modes, control, and voltage balancing," *IEEE Trans. Power Electron.*, vol. 33, no. 8, pp. 6537-6554, 2018.

- [23] Z. Shu, H. Lin, Z. Ziwei, X. Yin, and Q. Zhou, "Specific order harmonics compensation algorithm and digital implementation for multi-level active power filter," *IET Power Electron.*, vol. 10, no. 5, pp. 525-535, 2017.
- [24] Y. Hoon, M. A. M. Radzi, M. K. Hassan, and N. F. Mailah, "Operation of three-level inverter-based shunt active power filter under nonideal grid voltage conditions with dual fundamental component extraction," *IEEE Trans. Power Electron.*, vol. 33, no. 9, pp. 7558-7570, 2018.
- [25] M. S. Diab, A. M. Massoud, S. Ahmed, and B. W. Williams, "A dual modular multilevel converter with high-frequency magnetic links between submodules for MV open-end stator winding machine drives," *IEEE Trans. Power Electron.*, vol. 33, no. 6, pp. 5142-5159, 2018.
- [26] V. Nair, K. Gopakumar, and L. G. Franquelo, "A very high resolution stacked multilevel inverter topology for adjustable speed drives," *IEEE Trans. Ind. Electron.*, vol. 65, no. 3, pp. 2049-2056, 2018.
- [27] J. Dixon, J. Pereda, C. Castillo, and S. Bosch, "Asymmetrical multilevel inverter for traction drives using only one DC supply," *IEEE Trans. Veh. Technol.*, vol. 59, no. 8, pp. 3736-3743, 2010.
- [28] A. Joseph and T. R. Chelliah, "A review of power electronic converters for variable speed pumped storage plants: configurations, operational challenges, and future scopes," *IEEE Trans. Emerg. Sel. Topics Power Electron.*, vol. 6, no. 1, pp. 103-119, 2018.
- [29] A. Bocquel and J. Janning, "Analysis of a 300 MW variable speed drive for pump-storage plant applications," in *Proc. 11th Eur. Conf. on Power Electron. and Appl.*, 2005, pp. 1-10
- [30] M. V. Pronin, O. B. Shonin, A. G. Vorontsov, and G. A. Gogolev, "Features of a drive system for pump-storage plant applications based on the use of double-fed induction machine with a multistage-multilevel frequency converter," in *Proc. 15th Int. Power Electron. and Motion Contr. Conf.*, 2012, pp. 1-8
- [31] X. Zhang, T. Zhao, W. Mao, D. Tan, and L. Chang, "Multilevel inverters for grid-connected photovoltaic applications: examining emerging trends," *IEEE Power Electron. Mag.*, vol. 5, no. 4, pp. 32-41, 2018.
- [32] B. Xiao *et al.*, "Modular cascaded H-bridge multilevel PV inverter with distributed MPPT for grid-connected applications," *IEEE Trans. Ind. Appl.*, vol. 51, no. 2, pp. 1722-1731, 2015.
- [33] S. Daher, J. Schmid, and F. L. M. Antunes, "Multilevel inverter topologies for stand-alone PV systems," *IEEE Trans. Ind. Electron.*, vol. 55, no. 7, pp. 2703-2712, 2008.
- [34] M. M. Hasan, S. Mekhilef, and M. Ahmed, "Three-phase hybrid multilevel inverter with less power electronic components using space vector modulation," *IET Power Electron.*, vol. 7, no. 5, pp. 1256-1265, 2014.
- [35] A. Salem, E. M. Ahmed, M. Orabi, and M. Ahmed, "New three-phase symmetrical multilevel voltage source inverter," *IEEE Trans. Emerg. Sel. Topics Circuits Syst.*, vol. 5, no. 3, pp. 430-442, 2015.
- [36] F. Gao, "An enhanced single-phase step-up five-level inverter," *IEEE Trans. Power Electron.*, vol. 31, no. 12, pp. 8024-8030, 2016.
- [37] M. Nguyen and T. Tran, "Quasi cascaded H-bridge five-level boost inverter," *IEEE Trans. Ind. Electron.*, vol. 64, no. 11, pp. 8525-8533, 2017.

- [38] Y. Hu, Y. Xie, L. Cheng, and D. Fu, "Characteristics analysis of a new single-phase π -type five-level inverter," *IET Power Electron.*, vol. 9, no. 6, pp. 1290-1296, 2016.
- [39] Y. Hu, Y. Xie, D. Fu, and L. Cheng, "A new single-phase π -type 5-level inverter using 3-terminal switch-network," *IEEE Trans. Ind. Electron.*, vol. 63, no. 11, pp. 7165-7174, 2016.
- [40] S. Hashemizadeh-Ashan and M. Monfared, "Design and comparison of nine-level single-phase inverters with a pair of coupled inductors and two DC sources," *IET Power Electron.*, vol. 9, no. 11, pp. 2271-2281, 2016.
- [41] N. Sandeep and U. R. Yaragatti, "Design and implementation of a sensorless multilevel inverter with reduced part count," *IEEE Trans. Power Electron.*, vol. 32, no. 9, pp. 6677-6683, 2017.
- [42] N. Sandeep and U. R. Yaragatti, "Operation and control of an improved hybrid nine-level inverter," *IEEE Trans. Ind. Appl.*, vol. 53, no. 6, pp. 5676-5686, 2017.
- [43] H. K. Jahan, M. Naseri, M. M. Haji-Esmaceli, M. Abapour, and K. Zare, "Low component merged cells cascaded-transformer multilevel inverter featuring an enhanced reliability," *IET Power Electron.*, vol. 10, no. 8, pp. 855-862, 2017.
- [44] N. Sandeep and U. R. Yaragatti, "Design and implementation of active neutral-point-clamped nine-level reduced device count inverter: an application to grid integrated renewable energy sources," *IET Power Electron.*, vol. 11, no. 1, pp. 82-91, 2018.
- [45] N. Sandeep and U. R. Yaragatti, "Operation and control of a nine-level modified ANPC inverter topology with reduced part count for grid-connected applications," *IEEE Trans. Ind. Electron.*, vol. 65, no. 6, pp. 4810-4818, 2018.
- [46] J. P. R. A. Mello and C. B. Jacobina, "Single-phase converter with shared leg and generalizations," *IEEE Trans. Power Electron.*, vol. 33, no. 6, pp. 4882-4893, 2018.
- [47] A. Ahmed, M. S. Manoharan, and J. Park, "An efficient single-sourced asymmetrical cascaded multilevel inverter with reduced leakage current suitable for single-stage PV systems," *IEEE Trans. Energy Convers.*, vol. 34, no. 1, pp. 211-220, 2019.
- [48] J. Venkataramanaiah, Y. Suresh, and A. K. Panda, "Design and development of a novel 19-level inverter using an effective fundamental switching strategy," *IEEE Trans. Emerg. Sel. Topics Power Electron.*, vol. 6, no. 4, pp. 1903-1911, 2018.
- [49] S. Behara, N. Sandeep, and U. R. Yaragatti, "Design and implementation of transformer-based multilevel inverter topology with reduced components," *IEEE Trans. Ind. Appl.*, vol. 54, no. 5, pp. 4632-4639, 2018.
- [50] V. Jammala, S. Yellasiri, and A. K. Panda, "Development of a new hybrid multilevel inverter using modified carrier SPWM switching strategy," *IEEE Trans. Power Electron.*, vol. 33, no. 10, pp. 8192-8197, 2018.
- [51] A. A. Gandomi, S. Saaidabadi, S. H. Hosseini, E. Babaei, and Y. A. Gandomi, "Flexible transformer-based multilevel inverter topologies," *IET Power Electron.*, vol. 12, no. 3, pp. 578-587, 2019.
- [52] S. Behara, N. Sandeep, and U. R. Yaragatti, "Simplified transformer-based multilevel inverter topology and generalisations for renewable energy applications," *IET Power Electron.*, vol. 11, no. 4, pp. 708-718, 2018.

- [53] S. Salehahari, E. Babaei, S. H. Hosseini, and A. Ajami, "Transformer-based multilevel inverters: analysis, design and implementation," *IET Power Electron.*, vol. 12, no. 1, pp. 1-10, 2019.
- [54] H. K. Jahan, K. Zare, and M. Abapour, "Verification of a low component nine-level cascaded-transformer multilevel inverter in grid-tied mode," *IEEE Trans. Emerg. Sel. Topics Power Electron.*, vol. 6, no. 1, pp. 429-440, 2018.
- [55] J. Liu, J. Wu, J. Zeng, and H. Guo, "A novel nine-level inverter employing one voltage source and reduced components as high-frequency AC power source," *IEEE Trans. Power Electron.*, vol. 32, no. 4, pp. 2939-2947, 2017.
- [56] J. Zeng, J. Wu, J. Liu, and H. Guo, "A quasi-resonant switched-capacitor multilevel inverter with self-voltage balancing for single-phase high-frequency AC microgrids," *IEEE Trans. Ind. Inf.*, vol. 13, no. 5, pp. 2669-2679, 2017.
- [57] A. Taghvaie, J. Adabi, and M. Rezanejad, "Circuit topology and operation of a step-up multilevel inverter with a single DC source," *IEEE Trans. Ind. Electron.*, vol. 63, no. 11, pp. 6643-6652, 2016.
- [58] A. Taghvaie, J. Adabi, and M. Rezanejad, "A multilevel inverter structure based on a combination of switched-capacitors and DC sources," *IEEE Trans. Ind. Inf.*, vol. 13, no. 5, pp. 2162-2171, 2017.
- [59] C. Hsieh, T. Liang, S. Chen, and S. Tsai, "Design and implementation of a novel multilevel DC-AC inverter," *IEEE Trans. Ind. Appl.*, vol. 52, no. 3, pp. 2436-2443, 2016.
- [60] R. Barzegarkhoo, H. M. Kojabadi, E. Zamiry, N. Vosoughi, and L. Chang, "Generalized structure for a single phase switched-capacitor multilevel inverter using a new multiple DC link producer with reduced number of switches," *IEEE Trans. Power Electron.*, vol. 31, no. 8, pp. 5604-5617, 2016.
- [61] H. Samsami, A. Taheri, and R. Samanbakhsh, "New bidirectional multilevel inverter topology with staircase cascading for symmetric and asymmetric structures," *IET Power Electron.*, vol. 10, no. 11, pp. 1315-1323, 2017.
- [62] N. V. Kumar, V. K. Chinnaiyan, P. Murukesapillay, and S. P. Karthikeyan, "Multilevel inverter topology using single source and double source module with reduced power electronic components," *J. Eng.*, vol. 2017, no. 5, pp. 139-148, 2017.
- [63] S. A. A. Ibrahim, A. Palanimuthu, and M. A. J. Sathik, "Symmetric switched diode multilevel inverter structure with minimised switch count," *J. Eng.*, vol. 2017, no. 8, pp. 469-478, 2017.
- [64] R. S. Alishah, S. H. Hosseini, E. Babaei, and M. Sabahi, "Optimal design of new cascaded switch-ladder multilevel inverter structure," *IEEE Trans. Ind. Electron.*, vol. 64, no. 3, pp. 2072-2080, 2017.
- [65] L. Wang, Q. H. Wu, and W. Tang, "Novel cascaded switched-diode multilevel inverter for renewable energy integration," *IEEE Trans. Energy Convers.*, vol. 32, no. 4, pp. 1574-1582, 2017.
- [66] R. Samanbakhsh and A. Taheri, "Reduction of power electronic components in multilevel converters using new switched capacitor-diode structure," *IEEE Trans. Ind. Electron.*, vol. 63, no. 11, pp. 7204-7214, 2016.
- [67] S. S. Lee, B. Chu, N. R. N. Idris, H. H. Goh, and Y. E. Heng, "Switched-battery boost-multilevel inverter with GA optimized SHEPWM for standalone application," *IEEE Trans. Ind. Electron.*, vol. 63, no. 4, pp. 2133-2142, 2016.

- [68] N. Prabakaran, Z. Salam, C. Cecati, and K. Palanisamy, "Design and implementation of new multilevel inverter topology for trinary sequence using unipolar pulsewidth modulation," *IEEE Trans. Ind. Electron.*, vol. 67, no. 5, pp. 3573-3582, 2020.
- [69] S. Majumdar, B. Mahato, and K. C. Jana, "Implementation of an optimum reduced components multicell multilevel inverter (MC-MLI) for lower standing voltage," *IEEE Trans. Ind. Electron.*, vol. 67, no. 4, pp. 2765-2775, 2020.
- [70] L. He and C. Cheng, "A flying-capacitor-clamped five-level inverter based on bridge modular switched-capacitor topology," *IEEE Trans. Ind. Electron.*, vol. 63, no. 12, pp. 7814-7822, 2016.
- [71] S. Jain and V. Sonti, "A highly efficient and reliable inverter configuration based cascaded multilevel inverter for PV systems," *IEEE Trans. Ind. Electron.*, vol. 64, no. 4, pp. 2865-2875, 2017.
- [72] A. Kadam and A. Shukla, "A multilevel transformerless inverter employing ground connection between PV negative terminal and grid neutral point," *IEEE Trans. Ind. Electron.*, vol. 64, no. 11, pp. 8897-8907, 2017.
- [73] X. Sun *et al.*, "A single DC source cascaded seven-level inverter integrating switched-capacitor techniques," *IEEE Trans. Ind. Electron.*, vol. 63, no. 11, pp. 7184-7194, 2016.
- [74] H. Wu, L. Zhu, F. Yang, T. Mu, and H. Ge, "Dual-DC-port asymmetrical multilevel inverters with reduced conversion stages and enhanced conversion efficiency," *IEEE Trans. Ind. Electron.*, vol. 64, no. 3, pp. 2081-2091, 2017.
- [75] H. Wang, L. Kou, Y. Liu, and P. C. Sen, "A new six-switch five-level active neutral point clamped inverter for PV applications," *IEEE Trans. Power Electron.*, vol. 32, no. 9, pp. 6700-6715, 2017.
- [76] E. Samadaei, S. A. Gholamian, A. Sheikholeslami, and J. Adabi, "An envelope type (E-type) module: asymmetric multilevel inverters with reduced components," *IEEE Trans. Ind. Electron.*, vol. 63, no. 11, pp. 7148-7156, 2016.
- [77] S. Xu, J. Zhang, X. Hu, and Y. Jiang, "A novel hybrid five-level voltage-source converter based on T-type topology for high-efficiency applications," *IEEE Trans. Ind. Appl.*, vol. 53, no. 5, pp. 4730-4743, 2017.
- [78] M. Saeedian, J. Adabi, and S. M. Hosseini, "Cascaded multilevel inverter based on symmetric-asymmetric DC sources with reduced number of components," *IET Power Electron.*, vol. 10, no. 12, pp. 1468-1478, 2017.
- [79] K. Boora and J. Kumar, "General topology for asymmetrical multilevel inverter with reduced number of switches," *IET Power Electron.*, vol. 10, no. 15, pp. 2034-2041, 2017.
- [80] S. T. Meraj, K. Hasan, and A. Masaoud, "A novel configuration of cross-switched T-type (CT-type) multilevel inverter," *IEEE Trans. Power Electron.*, vol. 35, no. 4, pp. 3688-3696, 2020.
- [81] M. Khenar, A. Taghvaie, J. Adabi, and M. Rezanejad, "Multi-level inverter with combined T-type and cross-connected modules," *IET Power Electron.*, vol. 11, no. 8, pp. 1407-1415, 2018.
- [82] M. F. Kangarlu, E. Babaei, and M. Sabahi, "Cascaded cross-switched multilevel inverter in symmetric and asymmetric conditions," *IET Power Electron.*, vol. 6, no. 6, pp. 1041-1050, 2013.

- [83] S. S. Lee, C. S. Lim, and K. Lee, "Novel active-neutral-point-clamped inverters with improved voltage-boosting capability," *IEEE Trans. Power Electron.*, vol. 35, no. 6, pp. 5978-5986, 2020.
- [84] Y. P. Siwakoti, "A new six-switch five-level boost-active neutral point clamped (5L-Boost-ANPC) inverter," in *Proc. IEEE Appl. Power Electron. Conf. Expo.*, 2018, pp. 2424-2430
- [85] O. Husev, C. Roncero-Clemente, E. Romero-Cadaval, D. Vinnikov, and S. Stepenko, "Single phase three-level neutral-point-clamped quasi-Z-source inverter," *IET Power Electron.*, vol. 8, no. 1, pp. 1-10, 2015.
- [86] A. Ho and T. Chun, "Single-phase modified quasi-Z-source cascaded hybrid five-level inverter," *IEEE Trans. Ind. Electron.*, vol. 65, no. 6, pp. 5125-5134, 2018.
- [87] D. Sun *et al.*, "Modeling, impedance design, and efficiency analysis of quasi-Z source module in cascaded multilevel photovoltaic power system," *IEEE Trans. Ind. Electron.*, vol. 61, no. 11, pp. 6108-6117, 2014.
- [88] D. A. Ruiz-Caballero, R. M. Ramos-Astudillo, S. A. Mussa, and M. L. Heldwein, "Symmetrical hybrid multilevel DC-AC converters with reduced number of insulated DC supplies," *IEEE Trans. Ind. Electron.*, vol. 57, no. 7, pp. 2307-2314, 2010.
- [89] E. Gurpinar and A. Castellazzi, "Single-phase T-type inverter performance benchmark using Si IGBTs, SiC MOSFETS, and GaN HEMTs," *IEEE Trans. Power Electron.*, vol. 31, no. 10, pp. 7148-7160, 2016.
- [90] Q. Guan *et al.*, "An extremely high efficient three-level active neutral-point-clamped converter comprising SiC and Si hybrid power stages," *IEEE Trans. Power Electron.*, vol. 33, no. 10, pp. 8341-8352, 2018.
- [91] P. Knaup, "International patent application, nr. wo 2007/048420 A1," 2007.
- [92] M. Schweizer, I. Lizama, T. Friedli, and J. W. Kolar, "Comparison of the chip area usage of 2-level and 3-level voltage source converter topologies," in *Proc. 36th Annu. Conf. IEEE Ind. Electron. Soc.*, 2010, pp. 391-396
- [93] A. Salem and M. Abido, "T-type multilevel converter topologies: a comprehensive review," *Arabian J. Sci. Eng.*, vol. 44, no. 3, pp. 1713-1735, 2019.
- [94] U. Choi, F. Blaabjerg, and K. Lee, "Reliability improvement of a T-type three-level inverter with fault-tolerant control strategy," *IEEE Trans. Power Electron.*, vol. 30, no. 5, pp. 2660-2673, 2015.
- [95] M. Sahoo and S. Keerthipati, "A three-level LC-switching-based voltage boost NPC inverter," *IEEE Trans. Ind. Electron.*, vol. 64, no. 4, pp. 2876-2883, 2017.
- [96] V. F. Pires, A. Cordeiro, D. Foito, and J. F. Martins, "Quasi-Z-source inverter with a T-type converter in normal and failure mode," *IEEE Trans. Power Electron.*, vol. 31, no. 11, pp. 7462-7470, 2016.
- [97] A. Abdelhakim, P. Mattavelli, and G. Spiazzi, "Three-phase three-level flying capacitors split-source inverters: analysis and modulation," *IEEE Trans. Ind. Electron.*, vol. 64, no. 6, pp. 4571-4580, 2017.
- [98] P. C. Loh, F. Blaabjerg, and C. P. Wong, "Comparative evaluation of pulse-width modulation strategies for Z-source neutral-point-clamped inverter," in *Proc. 37th IEEE Power Electron. Spec. Conf.*, 2006, pp. 1-7
- [99] P. C. Loh, F. Gao, and F. Blaabjerg, "Topological and modulation design of three-level Z-source inverters," *IEEE Trans. Power Electron.*, vol. 23, no. 5, pp. 2268-2277, 2008.

- [100] A. Abdelhakim, P. Mattavelli, and G. Spiazzi, "Three-phase split-source inverter (SSI): analysis and modulation," *IEEE Trans. Power Electron.*, vol. 31, no. 11, pp. 7451-7461, 2016.
- [101] K. Wang, Z. Zheng, D. Wei, B. Fan, and Y. Li, "Topology and capacitor voltage balancing control of a symmetrical hybrid nine-level inverter for high-speed motor drives," *IEEE Trans. Ind. Appl.*, vol. 53, no. 6, pp. 5563-5572, 2017.
- [102] R. Agrawal and S. Jain, "Multilevel inverter for interfacing renewable energy sources with low/medium- and high-voltage grids," *IET Renewable Power Gener.*, vol. 11, no. 14, pp. 1822-1831, 2017.
- [103] M. Narimani, B. Wu, and N. R. Zargari, "A novel five-level voltage source inverter with sinusoidal pulse width modulator for medium-voltage applications," *IEEE Trans. Power Electron.*, vol. 31, no. 3, pp. 1959-1967, 2016.
- [104] Q. A. Le and D. Lee, "A novel six-level inverter topology for medium-voltage applications," *IEEE Trans. Ind. Electron.*, vol. 63, no. 11, pp. 7195-7203, 2016.
- [105] M. Narimani, B. Wu, Z. Cheng, and N. R. Zargari, "A new nested neutral point-clamped (NNPC) converter for medium-voltage (MV) power conversion," *IEEE Trans. Power Electron.*, vol. 29, no. 12, pp. 6375-6382, 2014.
- [106] R. Rojas, T. Ohnishi, and T. Suzuki, "PWM control method for a four-level inverter," *IEE Proc. Electr. Power Appl.*, vol. 142, no. 6, pp. 390-396, 1995.
- [107] A. Hota, S. Jain, and V. Agarwal, "A modified T-structured three-level inverter configuration optimized with respect to PWM strategy used for common-mode voltage elimination," *IEEE Trans. Ind. Appl.*, vol. 53, no. 5, pp. 4779-4787, 2017.
- [108] P. R. Kumar *et al.*, "A three-level common-mode voltage eliminated inverter with single DC supply using flying capacitor inverter and cascaded H-bridge," *IEEE Trans. Power Electron.*, vol. 29, no. 3, pp. 1402-1409, 2014.
- [109] R. R. Karasani, V. B. Borghate, P. M. Meshram, H. M. Suryawanshi, and S. Sabyasachi, "A three-phase hybrid cascaded modular multilevel inverter for renewable energy environment," *IEEE Trans. Power Electron.*, vol. 32, no. 2, pp. 1070-1087, 2017.
- [110] A. Hota, S. Jain, and V. Agarwal, "An optimized three-phase multilevel inverter topology with separate level and phase sequence generation part," *IEEE Trans. Power Electron.*, vol. 32, no. 10, pp. 7414-7418, 2017.
- [111] R. Raushan, B. Mahato, and K. C. Jana, "Comprehensive analysis of a novel three-phase multilevel inverter with minimum number of switches," *IET Power Electron.*, vol. 9, no. 8, pp. 1600-1607, 2016.
- [112] M. M. Hasan, A. Abu-Siada, and M. R. Islam, "Design and implementation of a novel three-phase cascaded half-bridge inverter," *IET Power Electron.*, vol. 9, no. 8, pp. 1741-1752, 2016.
- [113] V. Nair, A. Rahul, R. S. Kaarthik, A. Kshirsagar, and K. Gopakumar, "Generation of higher number of voltage levels by stacking inverters of lower multilevel structures with low voltage devices for drives," *IEEE Trans. Power Electron.*, vol. 32, no. 1, pp. 52-59, 2017.
- [114] S. Amamra, K. Meghriche, A. Cherifi, and B. Francois, "Multilevel inverter topology for renewable energy grid integration," *IEEE Trans. Ind. Electron.*, vol. 64, no. 11, pp. 8855-8866, 2017.

- [115] A. Salem, E. M. Ahmed, M. Orabi, and M. Ahmed, "Study and analysis of new three-phase modular multilevel inverter," *IEEE Trans. Ind. Electron.*, vol. 63, no. 12, pp. 7804-7813, 2016.
- [116] M. S. Mahdavi, G. B. Gharehpetian, Z. Mahdavi, and A. Keyhani, "Eighteen-step inverter; a low-loss three-phase inverter for low-cost standalone applications," *IEEE Trans. Emerg. Sel. Topics Power Electron.*, pp. 1-1, 2020.
- [117] Z. Shu, N. Ding, J. Chen, H. Zhu, and X. He, "Multilevel SVPWM with DC-link capacitor voltage balancing control for diode-clamped multilevel converter based STATCOM," *IEEE Trans. Ind. Electron.*, vol. 60, no. 5, pp. 1884-1896, 2013.
- [118] L. K. Haw, M. S. A. Dahidah, and H. A. F. Almurib, "SHE-PWM cascaded multilevel inverter with adjustable DC voltage levels control for STATCOM applications," *IEEE Trans. Power Electron.*, vol. 29, no. 12, pp. 6433-6444, 2014.
- [119] R. Sajadi, H. Iman-Eini, M. K. Bakhshizadeh, Y. Neyshabouri, and S. Farhangi, "Selective harmonic elimination technique with control of capacitive DC-link voltages in an asymmetric cascaded H-bridge inverter for STATCOM application," *IEEE Trans. Ind. Electron.*, vol. 65, no. 11, pp. 8788-8796, 2018.
- [120] B. Gultekin and M. Ermis, "Cascaded multilevel converter-based transmission STATCOM: system design methodology and development of a 12 KV \pm 12 MVar power stage," *IEEE Trans. Power Electron.*, vol. 28, no. 11, pp. 4930-4950, 2013.
- [121] C. J. Nwobu, I. B. Efika, O. J. K. Oghorada, and L. Zhang, "A modular multilevel flying capacitor converter-based STATCOM for reactive power control in distribution systems," in *Proc. 17th Eur. Conf. on Power Electron. and Appl.*, 2015, pp. 1-9
- [122] X. Liu, J. Lv, C. Gao, Z. Chen, and S. Chen, "A novel STATCOM based on diode-clamped modular multilevel converters," *IEEE Trans. Power Electron.*, vol. 32, no. 8, pp. 5964-5977, 2017.
- [123] A. Dekka, B. Wu, R. L. Fuentes, M. Perez, and N. R. Zargari, "Evolution of topologies, modeling, control schemes, and applications of modular multilevel converters," *IEEE Trans. Emerg. Sel. Topics Power Electron.*, vol. 5, no. 4, pp. 1631-1656, 2017.
- [124] A. F. Cupertino, J. V. M. Farias, H. A. Pereira, S. I. Seleme, and R. Teodorescu, "Comparison of DSCC and SDBC modular multilevel converters for STATCOM application during negative sequence compensation," *IEEE Trans. Ind. Electron.*, vol. 66, no. 3, pp. 2302-2312, 2019.
- [125] G. Farivar, C. D. Townsend, B. Hredzak, J. Pou, and V. G. Agelidis, "Low-capacitance cascaded H-bridge multilevel STATCOM," *IEEE Trans. Power Electron.*, vol. 32, no. 3, pp. 1744-1754, 2017.
- [126] H. Wang, M. Liserre, and F. Blaabjerg, "Toward reliable power electronics: challenges, design tools, and opportunities," *IEEE Industrial Electronics Magazine*, vol. 7, no. 2, pp. 17-26, 2013.
- [127] S. Yang *et al.*, "An industry-based survey of reliability in power electronic converters," *IEEE Trans. Ind. Appl.*, vol. 47, no. 3, pp. 1441-1451, 2011.
- [128] N. N. V. S. Babu and B. G. Fernandes, "Cascaded two-level inverter-based multilevel STATCOM for high-power applications," *IEEE Trans. Power Del.*, vol. 29, no. 3, pp. 993-1001, 2014.

- [129] V. F. Pires, A. Cordeiro, D. Foito, and J. F. Silva, "A STATCOM based on a three-Phase, triple inverter modular topology for multilevel operation," *IEEE Trans. Power Del.*, vol. 34, no. 5, pp. 1988-1997, 2019.
- [130] V. F. Pires, D. Foito, and J. F. Silva, "Fault-tolerant multilevel topology based on three-phase H-bridge inverters for open-end winding induction motor drives," *IEEE Trans. Energy Convers.*, vol. 32, no. 3, pp. 895-902, 2017.
- [131] M. R. Baiju, K. K. Mohapatra, R. S. Kanchan, and K. Gopakumar, "A dual two-level inverter scheme with common mode voltage elimination for an induction motor drive," *IEEE Trans. Power Electron.*, vol. 19, no. 3, pp. 794-805, 2004.
- [132] V. Khadkikar, "Enhancing electric power quality using UPQC: a comprehensive overview," *IEEE Trans. Power Electron.*, vol. 27, no. 5, pp. 2284-2297, 2012.
- [133] L. M. Tolbert, F. Z. Peng, and T. G. Habetler, "A multilevel converter-based universal power conditioner," *IEEE Trans. Ind. Appl.*, vol. 36, no. 2, pp. 596-603, 2000.
- [134] J. A. Munoz, J. R. Reyes, J. R. Espinoza, I. A. Rubilar, and L. A. Moran, "A novel multi-level three-phase UPQC topology based on full-bridge single-phase cells," in *Proc. 33th Annu. Conf. IEEE Ind. Electron. Soc.*, 2007, pp. 1787-1792
- [135] V. Muneer and A. Bhattacharya, "Cascaded H bridge multi level inverter based unified power quality conditioner," in *Proc. 8th Power India Int. Conf.*, 2018, pp. 1-6
- [136] V. R. Kota and S. Vinnakoti, "An artificial neural network based controller for MLC-UPQC with power angle adjustment," in *Proc. IEEE Reg. 10 Conf.*, 2017, pp. 250-255
- [137] L. Yunbo *et al.*, "MMC-UPQC: application of modular multilevel converter on unified power quality conditioner," in *Proc. IEEE Power Energy Soc. Gen. Meeting*, 2013, pp. 1-5
- [138] X. Xiangning, L. Jingjing, Y. Chang, and Y. Yongchun, "A 10kV 4MVA unified power quality conditioner based on modular multilevel inverter," in *Proc., Int. Electr. Mach. Drives Conf.*, 2013, pp. 1352-1357
- [139] L. Zhengfu *et al.*, "The start control strategy design of unified power quality conditioner based on modular multilevel converter," in *Proc., Int. Electr. Mach. Drives Conf.*, 2013, pp. 933-937
- [140] S. A. González and M. I. Valla, "UPQC implemented with cascade asymmetric multilevel converters," *Electr. Power Syst. Res.*, vol. 124, pp. 144-151, 2015.
- [141] Y. Siwakoti, A. Mahajan, D. Rogers, and F. Blaabjerg, "A novel seven-level active neutral point clamped converter with reduced active switching devices and DC-link voltage," *IEEE Trans. Power Electron.*, pp. 1-1, 2019.
- [142] N. Sandeep and U. R. Yaragatti, "A switched-capacitor-based multilevel inverter topology with reduced components," *IEEE Trans. Power Electron.*, vol. 33, no. 7, pp. 5538-5542, 2018.
- [143] R. Uthirasamy, V. K. Chinnaiyan, U. S. Ragupathy, and J. Karpagam, "Investigation on three-phase seven-level cascaded DC-link converter using carrier level shifted modulation schemes for solar PV system applications," *IET Renewable Power Gener.*, vol. 12, no. 4, pp. 439-449, 2018.
- [144] B. S. Naik, L. Umanand, K. Gopakumar, and B. S. Reddy, "A new two-phase five-level converter for three-phase isolated grid-tied systems with inherent

- capacitor balancing and reduced component count,” *IEEE Trans. Emerg. Sel. Topics Power Electron.*, vol. 6, no. 3, pp. 1325-1335, 2018.
- [145] B. S. Naik, L. Umanand, K. Gopakumar, and B. S. Reddy, “A two-phase five-level converter with least number of power switches requiring only a single DC source,” *IEEE Trans. Emerg. Sel. Topics Power Electron.*, vol. 6, no. 4, pp. 1942-1952, 2018.
- [146] J. Lee, H. Sim, J. Kim, and K. Lee, “Combination analysis and switching method of a cascaded H-bridge multilevel inverter based on transformers with the different turns ratio for increasing the voltage level,” *IEEE Trans. Ind. Electron.*, vol. 65, no. 6, pp. 4454-4465, 2018.
- [147] M. M. Hasan, A. Abu-Siada, and M. S. A. Dahidah, “A three-phase symmetrical DC-link multilevel inverter with reduced number of DC sources,” *IEEE Trans. Power Electron.*, vol. 33, no. 10, pp. 8331-8340, 2018.
- [148] V. F. Pires, D. Foito, and A. Cordeiro, “PV power conditioning system using a three-phase multilevel pulse width modulation inverter employing cascaded Scott transformers,” *IET Power Electron.*, vol. 12, no. 1, pp. 102-111, 2019.
- [149] S. K. Chattopadhyay and C. Chakraborty, “Three-phase hybrid cascaded multilevel inverter using topological modules with 1:7 ratio of asymmetry,” *IEEE Trans. Emerg. Sel. Topics Power Electron.*, vol. 6, no. 4, pp. 2302-2314, 2018.
- [150] M. Sahoo and S. Keerthipati, “Fault tolerant three-level boost inverter with reduced source and LC count,” *IET Power Electron.*, vol. 11, no. 2, pp. 399-405, 2018.
- [151] T. T. Davis and A. Dey, “Investigation on extending the DC bus utilization of a single-source five-level inverter with single capacitor-fed H-bridge per phase,” *IEEE Trans. Power Electron.*, vol. 34, no. 3, pp. 2914-2922, 2019.
- [152] M. G. Majumder *et al.*, “A five-level inverter scheme using single DC link with reduced number of floating capacitors and switches for open-end IM drives,” *IEEE Trans. Ind. Electron.*, pp. 1-1, 2019.
- [153] M. Norambuena, S. Kouro, S. Dieckerhoff, and J. Rodriguez, “Reduced multilevel converter: a novel multilevel converter with a reduced number of active switches,” *IEEE Trans. Ind. Electron.*, vol. 65, no. 5, pp. 3636-3645, 2018.
- [154] A. Karthik and U. Loganathan, “A reduced component count five-level inverter topology for high reliability electric drives,” *IEEE Trans. Power Electron.*, pp. 1-1, 2019.
- [155] A. K. Yadav *et al.*, “A hybrid 7-level inverter using low-voltage devices and operation with single DC-link,” *IEEE Trans. Power Electron.*, vol. 34, no. 10, pp. 9844-9853, 2019.
- [156] A. Kshirsagar *et al.*, “17-level inverter with low component count for open-end induction motor drives,” *IET Power Electron.*, vol. 11, no. 5, pp. 922-929, 2018.
- [157] A. Sheir, M. Z. Youssef, and M. Orabi, “A novel bidirectional T-type multilevel inverter for electric vehicle applications,” *IEEE Trans. Power Electron.*, vol. 34, no. 7, pp. 6648-6658, 2019.
- [158] M. d. Benedetto, A. Lidozzi, L. Solero, F. Crescimbin, and P. J. Grbović, “Five-level E-type inverter for grid-connected applications,” *IEEE Trans. Ind. Appl.*, vol. 54, no. 5, pp. 5536-5548, 2018.

- [159] M. M. Hasan, A. Abu-Siada, S. M. Islam, and M. S. A. Dahidah, "A new cascaded multilevel inverter topology with galvanic isolation," *IEEE Trans. Ind. Appl.*, vol. 54, no. 4, pp. 3463-3472, 2018.
- [160] B. S. Umesh and K. Sivakumar, "Dual-inverter-fed pole-phase modulated nine-phase induction motor drive with improved performance," *IEEE Trans. Ind. Electron.*, vol. 63, no. 9, pp. 5376-5383, 2016.
- [161] V. Nair, A. Rahul, S. Pramanick, K. Gopakumar, and L. G. Franquelo, "Novel symmetric six-phase induction motor drive using stacked multilevel inverters with a single DC link and neutral point voltage balancing," *IEEE Trans. Ind. Electron.*, vol. 64, no. 4, pp. 2663-2670, 2017.
- [162] A. C. N. Maia, C. B. Jacobina, N. B. d. Freitas, and I. R. F. M. P. d. Silva, "Open-end multilevel six-phase machine drive system with five three-leg converters," *IEEE Trans. Ind. Appl.*, vol. 53, no. 3, pp. 2271-2281, 2017.
- [163] B. P. Reddy, M. Rao, M. Sahoo, and S. Keerthipati, "A fault-tolerant multilevel inverter for improving the performance of a pole-phase modulated nine-phase induction motor drive," *IEEE Trans. Ind. Electron.*, vol. 65, no. 2, pp. 1107-1116, 2018.
- [164] M. S. Diab, A. A. Elserougi, A. M. Massoud, S. Ahmed, and B. W. Williams, "A hybrid nine-arm modular multilevel converter for medium-voltage six-phase machine drives," *IEEE Trans. Ind. Electron.*, vol. 66, no. 9, pp. 6681-6691, 2019.
- [165] B. P. Reddy and S. Keerthipati, "A multilevel inverter configuration for an open-end-winding pole-phase-modulated-multiphase induction motor drive using dual inverter principle," *IEEE Trans. Ind. Electron.*, vol. 65, no. 4, pp. 3035-3044, 2018.